Comparative and population genomics analyses of eared pheasants inhabiting highly varying altitudes

Siwen Wu[1,3†], Kun Wang[2,4†], Xuehai Ge[2†], Sisi Yuan[3], Dong-Dong Wu[4], Changrong Ge[2*], Junjing Jia[2*], Zhengchang Su[3*], Tengfei Dou[2*]

1. Institute of Medical Biology, Chinese Academy of Medical Sciences, Peking Union Medical College, Kunming, Yunnan, China.

2. Faculty of Animal Science and Technology, Yunnan Agricultural University, Kunming 650201, Yunnan, China.

3. Department of Bioinformatics and Genomics, College of Computing and Informatics, the University of North Carolina at Charlotte, Charlotte, NC 28223, USA.

4. State Key Laboratory of Genetic Resources and Evolution/Key Laboratory of Healthy Aging Research of Yunnan Province, Kunming Institute of Zoology, Chinese Academy of Sciences, Kunming, Yunnan, China.

†These authors contributed equally to this work.

*Corresponding author(s): Changrong Ge (gcrzal@126.com), Junjing Jia (junjingli2009@hotmail.com), Zhengchang Su (zcsu@uncc.edu), Tengfei Dou (tengfeidou@sina.com)

Abstract

Oxygen pressure varies dramatically with altitudes on Earth; however, humans and animals thrive at almost all altitudes. To better understand genetic basis underlying adaptation of closely related species to varying altitudes, we annotated and compared the genome of a white eared pheasant (WT) (*Crossoptilon crossoptilon*) inhabiting high altitudes and the genome of a brown eared pheasant (BR) (*C. mantchuricum*) inhabiting low altitudes. Moreover, we compared genetic variations in populations of WT and BR as well as of blue eared pheasants (BL) (*C. auritum*) inhabiting intermediate altitudes, and identified thousands of selective sweeps in each species. Intriguingly, the unique genes and pseudogenes in the two genomes converge on the same set of altitude adaptation-related pathways of four functional categories as genes in selective sweeps in each species. Thus, these species appear to adapt to highly varying altitudes by diverging selection on the same traits via loss-of-function mutations and fine-tuning genes in common pathways.

Introduction

Faunas have gone through an evolutionary process to gain physiological feature for the adaptation of highly varying oxygen abundance. Populations of humans[1-3] and many animal species that are naturally adapted to lowlands thrive in highland environments, such as Tibetan chickens[4-6], Tibetan pigs[7,8], Tibetan goats[9], Tibetan sheep[10,11], Tibetan mastiffs[12], Tibet cattle[13,14], ground tits[15], and yaks[16], to name a few. The major challenge faced by these populations of humans and animals in highland environments is the low oxygen pressure-induced stress on their physiological systems[17-19]. The long-term adaptation to low oxygen pressure environments has resulted in genetic changes in these human[1-3,14,17,20-27] and animal[4-7,10-16,19,28-31] populations. Adaptive mutations of many genes of humans[2,14,17,18,26,32,33] and animals[16,19,30,31,33,34] have been linked to highland environments. Moreover, introgression has been shown as a major mechanism for human[1,3,27] and domesticated animals[9,10,13] to adapt to highland environments. Despite these great progresses, the understanding of human and animal adaptation to highly varying altitudes is still limited[33]. Particularly, some closely related animal species can rapidly adapt to highly varying altitudes, thus, it is interesting to understand the genetic basis of their adaptation from low- to intermediate- and high-altitude environments.

Crossoptilon, belonging to the Phasianidae family in the Galliformes order, is a rare but important genus endemic in China[35]. There are four species in the *Crossoptilon* genus, including Tibetan eared pheasant (TB) (*C. harmani*), white eared pheasant (WT) (*C. crossoptilon*), blue eared pheasant (BL) (*C. auritum*) and brown eared pheasant (BR) (*C. mantchuricum*)[35,36]. These species are found in coniferous forests, mixed broadleaf-conifer forests and alpine scrubs in various parts of China with very different altitudes ranging from 800 m to 5,000 m[35,37-42]. TB and

WT are believed to be conspecifics, diverging about 0.5 million years ago[43]. They sympatrically inhabit montane forest at a high altitude of 3,000-5,000 m[35,36,38,40-42]. TB is distributed in southeastern Tibet and adjacent northern India (3,000-5,000 m)[35,38,41], while WT is found in Qinghai, Sichuan, Yunnan and Tibet (3,000-4,300 m)[35,40]. BL and BR are closely related, diverging about 0.3 million years ago[43], but allopatrically inhabit different areas[35,36]. BL is only encountered in the mountains of Qinghai, Gansu, Sichuan and Ningxia, at an intermediate altitude of 2,000-3,000 m[38,44], while BR is mainly distributed in mountains in Shanxi and Hebei and near Beijing, at an altitude of 800-2,600 m[37,39,42]. Thus, WT, BL and BR are excellent models to study the genetic basis for closely related species to adapt to highly varying altitudes.

Recently, Wang et al.[45] assembled a BR genome and re-sequenced three BR subpopulations and a BL population. Although they provide new insights into genomic changes during the course of BR's long-term population decline[45], genetic basis underlying the adaptation of the BR and BL to low (800-2,600 m) and intermediated altitudes (1500-3000 m), respectively, were not investigated. Moreover, with a small contig N50 (0.11 Mb), this BR genome assembly has limitations as a reference genome to study the *Crossoptilon* species. To fill the gap, we recently sequenced and assembled the genome of a WT individual at chromosome-level with a contig N50 of 19.6 Mb, and re-sequenced 10 WT individuals and a BL individual[46]. Combining our data in WT and BL[46] with those of Wang et al. in BL and BR[45], we were well positioned to investigate the genetic bases of these closely related avian species to adapt to highly varying altitudes using comparative and population genomics approaches. This study is based in part upon SW's dissertation[47].

Results

Annotation of protein-coding genes in the WT and BR genomes

To see whether gene contents are related to adaption of closely related avian species to different altitudes, we first annotated the assembled WT[46] and BR[45] genomes using a combination of reference- and RNA-based methods (Materials and Methods). Using the coding DNA sequences (CDSs) of 53 well-represented Aves (Table S1) as the templates and a total of 23 RNA-seq datasets from 20 tissues of WT individuals and three tissues of BR individuals (Materials and Methods), we annotated 16,377 and 15,410 protein-coding genes as well as 1,519 and 1,976 pseudogenes in the WT and BR genomes, respectively (Table 1). The vast majority (15,565 and 14,727) of these genes and all the pseudogenes (1,519 and 1,976) in the WT and BR genomes were predicted based on the CDSs in the reference genomes (reference-based), while a small portion (812 and 683) of the genes were predicted based on the RNA-seq datasets in the two species (RNA-based) (Table 1). To evaluate the effects of the unbalanced RNA-seq datasets on the numbers of annotated genes in the two genomes, we repeated the annotation process by 100 times with each time using the CDSs in the 53 Aves genomes for reference-based annotations and a total of six RNA-seq datasets for RNA-based annotation. Of the six RNA-seq datasets, three were those from the BR tissues and the other three were randomly selected in each annotation from the 20 datasets of the WT tissues. As shown in Table S2, in each of the 100 times of annotations, the total number of annotated genes in WT is larger than that in BR, which is mainly due to the larger number of genes annotated by the reference-based approach in WT (15,565) than in BR (14,727). On the other hand, the two genomes have a similar average number (350 vs 355) of genes annotated by the RNA-based approach (p-value = 0.33, two-tailed t-test). Interestingly, in 73 of the 100 times of annotations,

99 the BR genome has even more RNA-annotated genes than does the WT genome, suggesting
100 that the assembly quality of the CDSs in BR is good enough for finding genes. However, when
101 the union of the 100 annotations is taken, WT still has more RNA-based annotated genes (812
102 vs 683). Taken together, these results suggest that the difference in the numbers of genes in
103 the two species is not mainly due to the difference in the quality of genome assemblies and/or
104 the bias of RNA-seq datasets.

105 Most of the reference-based genes (14,815 and 14,518) in both species have an intact
106 open reading frame (ORF) (intact genes), while the remaining small numbers (750 and 209)
107 contain either premature stop codon or ORF-shift mutations, which are not supported by the
108 corresponding short DNA reads, we thus called them partially supported genes, as the
109 mutations might be caused by sequencing errors, particularly, in long reads. Vast majority of
110 the intact genes (99.01%), partially supported genes (97.73%), and pseudogenes (95.13%) in
111 WT were transcribed in at least one of the 20 tissues examined (Table S3). These percentages
112 (96.54%, 93.78% and 90.84%) are smaller in BR (Table S4) as RNA-seq data from only three
113 tissues are available[45]. Most (751 and 631) of the RNA-based genes in both species can be
114 mapped to the NT database[48] (NT-supported new genes), suggesting that they are likely true
115 genes. The remaining small numbers (61 and 52) that cannot be mapped to the NT database
116 are likely novel genes (Table 1).

117 We compared the RNA-based genes annotated in the WT and BR assemblies, and found
118 450 pairs with an identity > 96.8%, comprising 55.4% and 65.9% of their RNA-based genes,
119 respectively. They are likely true orthologous genes in both species, as the same patterns of
120 transcriptional noise are unlikely to occur in two different species. Moreover, most of the RNA-

121 based genes in both species (Tables S3 and S4) were varyingly expressed in different tissues
122 with RNA-seq data available (Figures 1a-1d), indicating that they might be authentic and
123 functional. In addition, we randomly selected 17 of the 812 RNA-based genes in WT and
124 measured their expression levels in 16 tissues using RT-qPCR. We found that 15 (88.24%) of
125 them were transcribed in at least one of the tissues and five of which were putative novel
126 genes (Table S5, Figure 1e), further suggesting that most of the RNA-based genes at least in WT
127 are likely authentic, although the expression patterns of some genes are different from those
128 seen in the RNA-seq data due probably to the different sensitivity of RT-qPCR and RNA-seq
129 methods (Figure 1f). Moreover, we annotated 12 and eight in WT and BR, respectively, of the
130 274 presumed missing genes in avian species[49] (Table S6).

131 **Most pseudogenes found in the WT and BR genomes are unprocessed and unitary and thus**
132 **might lose gene functions**

133 Vast majority (for WT, 1,310 or 86.2%; for BR, 1,701 or 86.1%) of pseudogenes in both WT and
134 BR genomes are unprocessed, i.e., they arose due to direct mutations in the parent genes. We
135 failed to find any functional copy of these unprocessed pseudogenes; thus, they are also
136 unitary[50]. To see whether the pseudogenization alleles in the 1,519 and 1,976 pseudogenes in
137 the WT and BR genomes, respectively, are under selection, we mapped the short reads from 10
138 WT individuals and 41 BR individuals to the corresponding genomes (Materials and Methods).
139 We found that most of the first pseudogenization alleles along the parental genes were fixed in
140 the population of the two species (Figures 2a and 2b), suggesting that these pseudogenization
141 events might be under positive selection and thus contribute to the phenotypic traits of the two
142 species. Interestingly, the synonymous mutations in true genes in the two species, which are

143 generally assumed to be selectively neutral, are largely uniformly distributed along the CDSs,
144 except at the two ends, where the numbers of synonymous mutations decrease (Figures 2c and
145 2d), consistent with an earlier report in chickens[51]. The reduced synonymous mutations at the
146 two ends of CDSs suggest that they might harbor functional elements not related to their
147 coding functions, such as transcriptional and post-transcriptional regulatory elements[52]. In
148 contrast, pseudogenization mutations are strongly biased to the 5'-ends and 3'-ends in both
149 species (Figures 2c and 2d). The same phenomenon was also found in the other species such as
150 human[51,53] and chickens[51]. Therefore, the strongly biased pseudogenization mutations to the 5'-
151 end and 3'-end in the two species also suggest that they are under positive selection.
152 Finally, of the 1,519 pseudogenes in the WT genome, 727 (47.9%) have alternative
153 transcripts, but only 10 (1.4%) have functional alternative transcripts (Table S7). Of the 1,976
154 pseudogenes in BR, 1,712 have alternative transcripts, but only 17 (1.0%) have functional
155 alternative transcripts (Table S8). These results suggest that most pseudogenes in both species
156 do not have functional alternative transcripts, further suggesting that most of them have lost
157 the functions of their parent genes.

158 **Unique genes and pseudogenes in WT and BR might be related to their adaptation to distinct**
159 **ecological niches**

160 We found that the WT and BR genomes shared 14,507 of their genes (88.6% and 94.1%) and
161 1,040 of their pseudogenes (68.5% and 52.6%) (Table 1). Meanwhile, the WT genome contains
162 1,870 unique genes and 479 unique pseudogenes, while the BR genome harbors 903 unique
163 genes and 936 unique pseudogenes (Tables S9-S12, Figure 3a). Of the 1,870 unique genes in the
164 WT genome, 658 (35.2%) are unique pseudogenes and 1,212 (64.8%) are missing in the BR

genome. Of the 936 unique pseudogenes in BR, 658 (70.3%) are unique genes and 278 (29.7%) are missing in the WT genome (Figure 3a). Moreover, of the 903 unique genes in the BR genome, 173 (19.2%) are unique pseudogenes and 730 (80.8%) are missing in the WT genome. Of the 479 unique pseudogenes in the WT genome, 173 (36.1%) are unique genes and 306 (63.9%) are missing in the BR genome (Figure 3a). There are a total of 3,357 genes that either are unique genes or become unique pseudogenes in the WT or BR genomes. To see whether the unique genes and pseudogenes in each species are related to their unique traits and reflect the evolutionary pressure received from their niches, we assigned GO terms to the unique genes and pseudogenes in each species based on their homologs in chickens or humans. The unique genes and pseudogenes in WT are involved in 69 and 25 biological pathways (Table S13), respectively, while those in BR are involved in 27 and 59 biological pathways, respectively (Table S13). Interestingly, the unique genes and pseudogenes with GO term assignments are mainly involved in and affect, respectively, pathways related to four major physiological functions: cardiovascular functions, energy metabolism, neuronal functions and immunity (Table S13, Figure 3b). It has been shown that alterations in these functions are critical for animals to adapt to different altitudes[33]. Thus, the unique genes and loss of functions of the missing genes and pseudogenes in BR and WT might play a role in the adaption of the two species to their strikingly different altitudes. A few examples of such genes and pseudogenes are given below.

1) Cardiovascular functions: As shown in Figure 3b, unique gene *PIK3C2G* in BR, which is pseudogenized in WT, is involved in the HIF (hypoxia-inducible factor) activation pathway[54-56]. Unique genes *SH2D2A*, *PRKCD*, *PRKD3* and *NOS3* in WT, which are all missing in BR, are involved

187 in the VEGF (vascular endothelial growth factor) signaling pathway that plays critical roles in
188 proliferation, survival and migration of blood endothelial cells required for the angiogenesis
189 pathway[57-59]. Unique genes *SH2D2A*, *MAP3K1*, *PRKCD*, *WNT1*, *PRKD3*, *NOS3*, *EPHA3*, *NOTCH1*
190 and *GRB14* in WT, which are missing (*SH2D2A*, *PRKCD*, *PRKD3*, *NOS3* and *EPHA3*) or
191 pseudogenized (*MAP3K1*, *WNT1*, *NOTCH1* and *GRB14*) in BR, are involved in the angiogenesis
192 pathway. Unique genes *DOK1* and *PIK3C2G* in BR, which are pseudogenized in WT, are involved
193 in the angiogenesis pathway. Unique genes *PRKCD*, *NOS3* and *NPR2* in WT are missing (*PRKCD*
194 and *NOS3*) or pseudogenized (*NPR2*) in BR, are involved in the endothelin signaling pathway.
195 Unique gene *ARRB1* in BR, which is missing in WT, is involved in the angiotensin II-stimulated
196 signaling through G proteins and beta-arrestin pathway. Unique gene *VWF* in WT, which is
197 pseudogenized in BR, is involved in blood coagulation pathway.
198 2) Energy metabolism: As shown in Figure 3b, unique gene *PFKM* in BR, which is
199 pseudogenized in WT, is involved in glycolysis. Unique genes *PRKCD*, *CACNB1* and *CACNB3* in
200 WT, which are missing (*PRKCD* and *CACNB3*) or pseudogenized (*CACNB1*) in BR, are involved in
201 the thyrotropin-releasing hormone receptor signaling pathway. Unique genes *IRS2* and *TSC2* in
202 WT, which are missing (*TSC2*) or pseudogenized (*IRS2*) in BR, are involved in the insulin/IGF
203 pathway-protein kinase B signaling cascade pathway. Unique gene *TSC2* in WT, which is missing
204 in BR, is involved in the p53 pathway by glucose deprivation.
205 3) Neuronal functions: As shown in Figure 3b, unique genes *CACNA1D*, *CACNB1* and
206 *CACNB3* in WT, which are missing (*CACNA1D* and *CACNB3*) or pseudogenized (*CACNB1*) in BR,
207 are members of the beta1/2 adrenergic receptor signaling pathway. Unique gene *ADRB1* in BR,
208 which is pseudogenized in WT, is involved in the beta1/2 adrenergic receptor signaling pathway.

209 Unique genes *GRIK1* and *GRIN2C* in WT, which are pseudogenized in BR, are involved in the
210 metabotropic glutamate receptor group I pathway. Unique gene *CACNB1* (metabotropic
211 glutamate receptor group III pathway) in WT is pseudogenized in BR. Unique gene *GABBR1*
212 (GABA-B receptor II signaling pathway) in WT is missing in BR. Unique genes *CAMK2G*, *GRIK1*,
213 *SHANK2*, *GRIN2C* and *CAMK2B* in WT, which are missing (*SHANK2* and *CAMK2B*) or
214 pseudogenized (*CAMK2G*, *GRIK1* and *GRIN2C*) in BR, are involved in the ionotropic glutamate
215 receptor pathway. Unique genes *CACNA1D*, *MYO15A* and *CACNB1* in WT, which are missing
216 (*CACNA1D*) or pseudogenized (*MYO15A*, *CACNB1*) in BR, are involved in the nicotinic
217 acetylcholine receptor signaling pathway.

218 4) Immunity: As shown in Figure 3b, unique gene *MAP3K1* in WT, which is
219 pseudogenized in BR, is involved in the T cell activation pathway. Unique gene *PIK3C2G* in BR,
220 which is pseudogenized in WT, is involved in the T cell activation pathway. Unique genes *CD79A*
221 and *PRKCD* in WT, which are missing in BR, are involved in the B cell activation pathway. Unique
222 genes *PREX1*, *CAMK2G*, *ITGB7*, *VWF*, *TYK2*, *IL6* and *CAMK2B* in WT, which are missing (*ITGB7*,
223 *VWF*, *TYK2* and *CAMK2B*) or pseudogenized (*PREX1*, *CAMK2G*, *VWF* and *IL6*) in BR, are members
224 of the inflammation mediated by chemokine and cytokine signaling pathway. Unique gene
225 *ARRB1* in BR, which is missing in WT is involved in inflammation mediated by chemokine and
226 cytokine signaling pathway.

227 In addition, some unique genes or unique pseudogenes in the two species are involved
228 in pathways that might be related to the adaptation of the two species to other aspects of their
229 distinct ecological niches. For example, unique genes *CACNA1D*, *PRKCD*, *CACNB1* and *CACNB3* in
230 WT are missing (*CACNA1D*, *PRKCD* and *CACNB3*) or pseudogenized (*CACNB1*) in BR (Table S13).

231 These genes are involved in oxytocin receptor mediated signaling pathway that has been shown
232 to play critical roles in social behaviors of animals[60]. Moreover, unique genes *IRS2*, *SMAD4*,
233 *FOSB*, *CACNA1D*, *MAP3K1*, *PRKCD*, *MAP2K7*, *EP300*, *NR5A1*, *NPR2*, *MAP3K5* and *CAMK2B* in WT
234 are missing (*SMAD4*, *FOSB*, *CACNA1D*, *PRKCD*, *MAP2K7*, *NR5A* and *CAMK2B*) or pseudogenized
235 (*IRS2*, *MAP3K1*, *EP300*, *NPR2* and *MAP3K5*) in BR (Table S13), these genes are in involved in
236 gonadotropin releasing hormone receptor pathway that regulate reproduction.

237 **The populations of the three species are strongly structured**

238 To further understand the genetic basis of altitude adaptation, we next compared the SNPs of
239 10 WT individuals, 41 BR individuals and 12 BL individuals (Table 2). Figure 4a shows the
240 geographical locations where the populations were sampled. Specifically, the three BR
241 subpopulations were from Shaanxi province, Shanxi province, and Hebei province & Beijing
242 metropolitan, respectively[45]; the BL population were from Gansu province[45]; and the WT
243 population were from Yunnan province. Using our assembled WT genome[61] as the reference,
244 we identified SNPs in the BL, BR and WT populations (Table 2). Based on the bi-allelic SNPs (16
245 million) in the populations of the three species (Table 2), we performed principal component
246 analysis (PCA), and found that individuals of the same species form distinct clusters (Figure 4b).
247 Notably, each of the three BR subpopulations forms a distinct compact subcluster, which is
248 consistent with the previous result[45]. We also run the admixture algorithm[62] on the SNPs to
249 infer their ancestral relationships. For K=2, individuals of BL and BR formed a uniformly colored
250 cluster, while WT individuals formed the other cluster sharing small portions of ancestries with
251 the former two species (Figure 4c), suggesting that BL and BR were derived from the same
252 ancestor, while WT branched out earlier. This result is consistent with previous phylogenetic

analysis that BL and BR are more closely related to each other[43]. For K=3, individuals of each species formed an almost uniformly colored cluster, indicating their distinct recent ancestries.

To see possible gene introgression among the three species, we calculated the D-statistic[63] and f3-statistic[64]. We obtained a D value of 0.57 (z-score = 36.18, and p-value= 2.3e-16) using a Daweishan chicken population as the outgroup (O) on the rooted tree (((BR,BL),WT),O), suggesting introgression between BL and WT[63]. The f3 values and associated z-scores for the three choices of (target; source 1, source 2) are shown in Table 3. The significant (z-score = -26.45) negative f3 value (-0.0586) for (target=BL; source 1 = WT, source 2 = BR) suggests introgression in BL from both WT and BR[64]. However, the positive f3 values for the other two scenarios (Table 3) could not indicate there is gene introgression in BR from WT and BL, and in WT from BR and BL[64]. Thus, although gene introgression might have occurred in BL from both BR and WT, the data does not support gene introgression in BR from WT and BL, and in WT from BR and BL. Thus, gene introgression might play a role in the evolution of BL, but this might not be the case for BR and WT.

Genes in selective sweeps of each species might be related to their distinct ecological niches

To identify genomic regions and genes that might be related to the adaptation of the three species to their distinct ecological niches, particularly, to different altitudes, we identified selective sweeps in each species by comparing its SNPs with those of the other two species using both the genetic differentiation (F_{ST}) and difference in nucleotide diversity ($\Delta\pi$) parameters[65-68]. To rigorously evaluate the statistical significance of the F_{ST} and $\Delta\pi$ values, we normalized them (ZF_{ST} and $Z\Delta\pi$) using a permutation test[69] (Materials and Methods). Figures 5a-5c show the distribution of ZF_{ST} and $Z\Delta\pi$ as well as their values for each 40 kb genome

275 windows with a 20 kb-step size for the three pairwise comparisons. We consider a window with
276 ZF_{ST} > 2.33 (P=0.01) and $Z\Delta\pi$ > 1.64 (P=0.05) or $Z\Delta\pi$ < -1.64 (P=0.05) as a selective sweep
277 (Figures 5a-5c). Figures 6a-6f show the Manhattan plots of ZF_{ST} and $Z|\Delta\pi|$ scores for the three
278 pairwise comparisons. Since adjacent selective sweeps can overlap with one another, we
279 merged the overlapping ones as a discrete selection sweep (DSS) in each species. For the BL vs
280 BR comparison, we identified 208 and 638 selective sweeps, and 128 and 463 DSSs containing
281 143 and 474 genes in BL and BR, respectively (Tables 4 and S14). For the BL vs WT comparison,
282 we identified 92 and 274 selective sweeps, and 72 and 181 DSSs containing 67 and 167 genes in
283 BL and WT, respectively (Tables 4 and S15). For the BR vs WT comparison, we identified 306
284 and 359 selective sweeps, and 184 and 188 DSSs containing 196 and 167 genes in BR and WT,
285 respectively (Tables 4 and S16).

286 To further confirm our identified selective sweeps, we computed Tajima's D values for
287 each 40 kb window. As shown in Figures 6g-6i and Table S17, BR has the largest number (38,488)
288 of windows with positive Tajima's D values among the three species, suggesting that BR has
289 experienced a large-scale population contraction, consistent with the previous report[45]. For BL
290 and WT, most of their selective sweeps identified above in each pair-wise comparison (78.8%,
291 53.3%, 90% and 87.2% for BL vs BR, BL vs WT, BL vs WT and BR vs WT, respectively) have a
292 negative Tajima's D value (Table S17), suggesting negative or positive selections and confirming
293 the selective sweeps identified above.

294 To find the duration and intensity of the selective sweep in each species, we calculated
295 the run of homozygosity (ROH) in each selective sweep for each pair of comparison. As shown
296 in Figures 6j-6l and Table S17, BR has the largest number of selective sweeps (66.7%-70.5%)

297 with a high ratio of individuals that have a long ROH (>100kb), suggesting that BR has the most
298 recent inbreeding, their selection sweeps arose recently, and the selection intensity of BR is the
299 largest compared to the other two species. By contrast, both BL and WT have only small
300 portions (12%-16.8%) of selective sweeps with a long ROH (Table S17). These results suggest
301 that BR has undergone the most intensive selection recently compared to BL and WT, which is
302 consistent with the previous report[45].

303 To see whether genes in the selective sweeps are under positive or negative selections,
304 we calculated the ratio of the number of nonsynonymous mutations over the number of
305 synonymous mutations (dN/dS) for each gene in the DSSs for each pair of comparison. As
306 shown in Table S17, of the genes in the identified DSSs in each pair of comparison, 76.1-90.4%
307 are under purifying selection (dN/dS<1), while 6.6-19.4% are under positive selection (dN/dS>1).
308 Thus, most (90.5-97.6%) of the genes in the identified DSSs are under selection.

309 Genes in the DSSs of each comparison might be related to adaptation to their different
310 ecological niches. About 55% of genes in these selective sweeps identified in each comparison
311 do not harbor fixed nonsynonymous mutations, thus, natural selection might act upon their
312 regulatory sequences, thereby changing their expression levels. The remaining about 45% of
313 the genes contain fixed nonsynonymous mutations that might alter the functions of encoded
314 proteins. For example, gene *MYO3B* is located in a selective sweep in the BR population based
315 on the BL vs BR comparison (Figure 5a). *MYO3B* in BR contains a fixed G-to-A nonsynonymous
316 mutation in exon 7, leading to an Arg-to-Lys substitution. Since the AGA codon for Arg at this
317 position in *MYO3B* is shared by WT, BL, quail (*Coturnix japonica*) and human (*Homo sapiens*)
318 (Figure 5d), the G-to-A mutation is BR lineage specific. Thus, the Arg-to-Lys substitution in

319 *MYO3B* in BR might be related to their unique traits. It is reported that gene *MYO3B* is required
320 for normal cochlear hair bundle development and hearing[70]. As BR has been hunted by human
321 for hundreds of years[48], it is highly likely that the mutation might increase their auditory
322 sensation, thereby helping them to escape earlier when perceiving hunters approaching. It is
323 interesting to investigate the effects of the Arg-to-Lys mutation on the auditory functions of BR
324 and its implication for natural selection and adaptation. Moreover, gene *PTPRC* is located in a
325 selective sweep in the WT populations based on both the BL vs WT and the BR vs WT
326 comparisons. *PTPRC* in WT contains a fixed A-to-G nonsynonymous mutation in exon 7,
327 resulting in a Lys-to-Arg substitution. As the AAA codon for Lys at the position in *PTPRC* is
328 shared by BL, BR, quail and human (Figure 5d), the mutation is WT lineage specific. Interestingly,
329 we found that the same mutation existed in the *PTPRC* genes of Lance-tailed manakin
330 (*Chiroxiphia lanceolata*) and White-ruffed manakin (*Corapipo altera*) (Figure 5d), both are
331 altitudinal migrants living in subtropical Andes highlands[71], due probably to convergent
332 evolution. It has been reported that *PTPRC* is related to the T cell activation[72]. Therefore, it is
333 highly likely that the nonsynonymous mutation in the *PTPRC* gene in WT and manakins might
334 help them adapt to high altitudes where there are fewer pathogens, and thus, the pressure on
335 the immune system in these species might be relaxed.

336 **Genes under selection tend to be involved in the same altitude adaptation-related pathways**
337 **in the three species**

338 There are a total of 1,106 genes that are in a selective sweep predicted based on at least one of
339 the three comparisons. They share only 105 genes with the 3,357 unique genes and
340 pseudogenes in the WT and BR genomes (Figure 7a). Intriguingly, the genes with GO term

assignments in the selective sweeps in each species tend to be involved in the same pathways in the four functional categories (Tables S14-S16) as are the unique genes and unique pseudogenes with GO term assignments in the WT and BR genomes (Table S13), although the two sets only share four genes (Figure 7b). For example, selection on cardiovascular function-related genes *MAPK1* and *PRKAR2B* in BL might be related to its adaptation to intermediate altitudes, while selection on neuronal function related gene *PRKAR2B* might be beneficial for BL to survive in its ecological niches (Figure 7b). Moreover, selection on cardiovascular (*PLA2G4A*), immunity (*ITPR2*), energy metabolism (*PRKCD*) and neuronal function (*SLC17A6*) related genes might be beneficial for BR to adapt to low altitude (Figure 7b). Furthermore, selection on the hypoxia response (*PPARG*) related genes might help WT to adapt to the high-altitude niches, while selection on immunity (*PPP3CB*, *MAPK8* and *PTPRC*) and neuronal function (*GRIN3A*) related genes might be beneficial for WT to adapt to their unique ecological niches (Figure 7b). More examples of genes in the selective sweeps, which are involved in altitude-adaptation related pathways, are given as follows.

For BL, genes in selective sweeps identified in the BL vs BR and BL vs WT comparisons are involved in the same number of 22 GO pathways (Table 4). Compared to BR, six genes in the selection sweeps in BL have GO pathway assignments (Table S14). Among these genes, *MAPK1* is involved in cardiovascular functions such as angiogenesis pathway, VEGF signaling pathway[57-59], endothelin signaling pathway[73-75], and angiotensin II-stimulated signaling through G proteins and beta-arrestin pathway (Figure 7b). Compared to WT, 76 genes in the selection sweeps in BL have GO pathway assignments (Table S15). Among these genes, *PRKAR2B* is involved in neuronal functions such as beta1/2 adrenergic receptor signaling pathway, metabotropic

363 glutamate receptor group III pathway, GABA-B receptor II signaling pathway and endothelin
364 signaling (Figure 7b).
365 For BR, genes in the selective sweeps identified in the BL vs. BR and BR vs WT
366 comparisons are involved in 27 and 32 GO pathways, respectively (Table 4). Compared to BL,
367 175 genes in the selection sweeps in BR have GO pathway assignments (Table S14). Among
368 these genes, some are involved in cardiovascular functions, such as *PLA2G4A* (VEGF pathway
369 and angiogenesis pathway), *PLA2G4A* and *ITPR2* (endothelin signaling pathway), *ITPR2*
370 (angiotensin II-stimulated signaling through G proteins & beta-arrestin pathway), *PLA2G4A*
371 (oxidative stress response pathway); some are involved in immunity such as *PLA2G4A* and
372 *ITPR2* (B cell activation pathway); some are involved in neuronal functions, such as *RYR2*
373 (beta1/2 adrenergic receptor signaling pathway), *SLC17A6* (ionotropic glutamate receptor
374 pathway) (Figure 7b). Compared to WT, 78 genes in the selection sweeps in BR have GO
375 pathway assignment (Table S16). Some of these genes are involved in cardiovascular functions,
376 such as *PRKCD* (VEGF pathway, angiogenesis pathway, endothelin signaling pathway) that is
377 missing in the selection sweep in BR. *PRKCD* is also involved in energy metabolism (thyrotropin-
378 releasing hormone receptor signaling pathway), immunity (B-cell activation pathway) and
379 neuronal functions (alpha adrenergic receptor signaling pathway) (Figure 7b). Moreover,
380 *PRKAR2B* is also under selection in BR, which is involved in neuronal functions (Figure 7b).
381 For WT, genes in the selective sweeps identified in the BL vs WT and BR vs WT
382 comparisons are involved in 62 and 48 GO pathways, respectively (Table 4). Compared to BL,
383 341 genes in the selection sweeps in WT have GO pathway assignments (Table S15). Of these
384 genes, some are involved in cardiovascular functions such as *ARNT2* and *PPARG* (hypoxia

385 induced factor pathway[54-56,76]), *FZD1* and *MAPK8* (angiogenesis pathway) and *MAPK8* (oxidative
386 stress response pathway); some are involved in energy metabolism pathway, such as *PPP2CB*
387 (p53 pathway by glucose deprivation); some are involved in neuronal functions, such as *GRIN3A*
388 (metabotropic glutamate receptor group I pathway, metabotropic glutamate receptor group III
389 pathway and ionotropic glutamate receptor pathway) and *GABBR2* (GABA-B receptor II
390 signaling pathway); and some are involved in immunity, such as *PPP3CB*, *MAPK8* and *PTPRC*
391 (T/B cell activation pathway), *MAPK8* and *UBE2V1* (toll receptor signaling pathway and
392 interferon-gamma signaling pathway) (Figure 7b).
393 Moreover, compared to BR, 254 genes in the selection sweeps in WT have GO pathway
394 assignments (Table S16). Of the these genes, some are involved in cardiovascular functions,
395 such as *MAPK8* (oxidative stress response pathway[77-81]), *TEK*, *FZD1* and *MAPK8* (angiogenesis
396 pathway), and *VWF* (blood coagulation pathway) that is missing in BR (Figure 3b); Some are
397 involved in immunity, such as *MAPK8* (interferon-gamma signaling pathway and toll receptor
398 signaling pathway), *PPP3CB*, *MAPK8* and *PTPRC* (T/B cell activation pathway and toll receptor
399 signaling pathway and interferon-gamma signaling pathway[82-84]), *CAMK2G* (pseudogenized in
400 BR) and *VWF* (inflammation mediated by chemokine and cytokine signaling pathway[85,86]); some
401 are involved in neuronal functions, such as *GRIN3A* (metabotropic glutamate receptor group I
402 pathway, metabotropic glutamate receptor group III pathway), *GABBR2* (GABA-
403 B_receptor_II_signaling pathway), *CAMK2G* and *GRIN3A* (ionotropic glutamate receptor
404 pathway) (Figure 7b).
405
406 **Discussion**

407 To better understand the genetic bases of adaptation of closely related eared pheasant species
408 to highly varying altitudes, we combined our own published data in WT and BL[46] with those in
409 BR and BL published by Wang et al.[45]. We first annotated the assembled WT[46] and BR[45]
410 genomes, and compared their gene compositions. We identified similar numbers of protein-
411 coding genes in the WT (16,447) and BR (15,410) genomes to those annotated in other avian
412 species[87], but surprisingly large numbers of pseudogenes in them (1,519 in WT and 1,976 in BR),
413 not previously reported in other avian genomes, to our best knowledge. We provided evidence
414 that most pseudogenization mutations are under positive selection and the resulting
415 pseudogenes might have lost gene functions.

416 We found that many unique genes in one species (WT or BR) are often either missing or
417 pseudogenized in the other species (BR or WT). Interestingly, these unique genes and genes
418 with loss-of-function mutations (pseudogenization or missing) are mainly involved in and affect,
419 respectively, pathways related to four functional categories: cardiovascular, neuronal, energy
420 metabolic, and immune functions. This finding is quite interesting but not very surprising, since
421 cardiovascular, neuronal, and metabolic functions are highly sensitive to blood oxygen levels
422 which is directly affected by oxygen pressures at varying altitudes. Moreover, varying
423 pathogens and ultraviolet radiations at varying altitudes might require different immune
424 responses to infections and DNA damages. Physiological systems often contain both positive
425 and negative regulatory pathways to achieve a homeostasis of the functions. Thus, both the
426 presence of a gene involved in the positive pathway and the loss of a gene involved in the
427 negative pathway can enhance the relevant function. Conversely, both the presence of a gene
428 involved in the negative pathway and the loss of gene involved in positive pathway can

429 suppress the relevant functions. More specifically, the presence or the loss of genes in WT
430 might lead to changes in these four functional categories that are beneficial to its adaptation to
431 high altitude, as have been reported for other high-altitude adapted species and populations of
432 humans and animals[4,7,11,15,18,19,22,23,31]. And the loss or the presence of the same genes in BR
433 might lead to opposite changes of these four functional categories that are beneficial to its
434 adaptation to low altitude. For example, we found that gene *PIK3C2G* in BR is pseudogenized in
435 WT. This gene is involved in many pathways, including the HIF pathway, endothelin signaling
436 pathway, angiogenesis pathway, VEGF signaling pathway, T cell activation pathway and
437 inflammation mediated by chemokine and cytokine signaling pathway (Figure 3b). It is likely
438 that functional *PIK3C2G* in BR plays a role in BR's possibly low demands for these cardiovascular
439 and immune functions to adapt to low altitudes, while the loss-of-function of *PIK3C2G* in WT
440 might better meet WT's possibly high demands for these functions to adapt to high altitudes.
441 Moreover, gene *CACNB1* in WT is pseudogenized in BR. This gene is involved in the beta1/2
442 adrenergic receptor signaling pathway, metabotropic glutamate receptor group III pathway,
443 nicotinic acetylcholine receptor signaling pathway and thyrotropin-releasing hormone receptor
444 signaling pathway (Figure 3b). It is likely that functional *CACNB1* in WT might play a role in WT's
445 possibly high demands for these neuronal and energy metabolic functions to adapt to high
446 altitudes or other aspects of its unique niches, while the loss-of-function of *CACNB1* in BR might
447 better meet BR's possibly low demands for these functions to adapt to low altitudes or other
448 aspects of its unique niches.

449 Next, we compared the SNPs in the WT, BL and BR populations. Interestingly, we found
450 that genes in the selective sweeps in each species are mainly involved in the same GO pathways

451 of the four functional categories as are the unique genes and pseudogenes in the WT and BR
452 genomes, even though the two sets of genes have little overlaps (Figure 7a). Most genes in the
453 selective sweeps do not have amino acid-altering mutations, although some may have missense
454 mutations such as *MYO3B* in BR and *PTPRC* in WT (Figure 5d), become pseudogenes such as
455 *CACNB2*, or be missing such as *PRKCD* in BR. These results suggest that natural selection might
456 act on their *cis*-regulatory sequences, thereby altering their expression levels in relevant tissues.
457 It appears that natural selection on these genes might be related to the adaptation of the
458 species to different niches, particularly different altitudes. For example, in the BL vs BR
459 comparison, gene *MAPK1* in BL is included in a selective sweep. This gene is involved in the
460 VEGF signaling pathway, angiogenesis pathway, endothelin signaling pathway, angiotensin II-
461 stimulated signaling through G proteins and beta-arrestin pathway, insulin/IGF pathway-
462 mitogen activated protein kinase kinase/MAP kinase cascade pathway, and many pathways of
463 the immunity (Figure 7b). It is likely that selection on *MAPK1* might be related to the adaptation
464 of BL to intermediate altitude. In the WT vs BL comparison, gene *PPARG* is included in a
465 selective sweep, and the gene is involved in the HIF pathway[76] (Figure 7b), thus, selection on
466 the gene might be related to the adaptation of WT to low oxygen pressure at high altitudes.
467 It is not surprising that the unique genes/pseudogenes in WT and BR and genes in the
468 selective sweeps of BL, BR and WT converge on the same sets of pathways involved in
469 cardiovascular, energy metabolic, neuronal and immune functions. On the one hand, high
470 altitude niches with low oxygen pressure, low temperature and less availability of food would
471 pose a direct pressure on WT's cardiovascular system and energy metabolism functions, while
472 such pressure would be somewhat relaxed on BL and even more relaxed on BR. On the other

473 hand, other altitude related ecological factors might exert different pressures on the three
474 species for their neuronal functions for food foray and escaping for predators, and for immune
475 functions for different pathogens at varying altitudes. Indeed, it has been shown that high
476 altitude niches can have effects on the neuronal functions such as sensory perception in
477 domestic yaks (*Bos grunniens*)[16], and olfaction in Tibetan pig[7], wild boars[7] and ground tit (*Parus*
478 *humilis*)[15]. In this study, we found that a nonsynonymous mutation in *MYO3B* in the BR
479 population might alter their auditory sensation. It has also been shown that high altitude niches
480 can have effects on immune functions in ground tit[15]. In this study, we found that a
481 nonsynonymous mutation in *PTPRC* in the WT population and Manakins might alter their T-cell
482 functions. Thus, it appears that the three eared pheasant species might adapt to highly varying
483 altitudes or other aspects of their distinct ecological niches by loss-of-function mutations and
484 fine-tuning genes involved in the same set of pathways to meet their varying demands for the
485 four major functions. In other words, genes in this set of pathways might play roles in the
486 adaptation of the three pheasant species to different niches, particularly, different altitudes by
487 complete deletion (gene missing), pseudogenization, alteration of CDSs, or alteration of *cis*-
488 regulatory sequences.
489 Finally, to our best knowledge, we provided thus far the most comprehensive
490 annotation of genes and pseudogenes in the WT and BR genomes. We also identified numerous
491 selection sweeps in the WT, BR, and BL genomes. These results can be valuable resources for
492 researchers to better understand the biology of these uniquely adapted species and for policy
493 makers to design strategies for the preservation of these endangered species.
494

Materials and Methods

Datasets

We downloaded our previously published data[46], including the assembled genome of the WT individual from GenBank with accession number GCA_036346035.1, re-sequencing data of 10 WT individuals from NCBI SRA with accession number SRP433016, re-sequencing data of a BL individual from NCBI SRA with accession number SRP471294, and RNA-seq data from 20 tissues (chest muscle, leg muscle, liver, kidney, lung, spleen, heart, cerebellum, brain cortex, ovary, glandular, pancreas, abdominal fat, skin from chest, crops, rectum, cecum, duodenum, small intestine and gizzard) of the WT individual from NCBI SRA with accession number SRP432961. We downloaded the published datasets[45], including the assembled genome of the BR individual from China National Genomics Data Center (CNGDC) with accession number GWHAOPW00000000, re-sequencing data of 41 BR individuals from CNGDC with project number PRJCA003284, RNA-seq data from three BR tissues (blood, developing primaries, and developing tail feathers) from CNGDC with project number PRJCA003284, and re-sequencing data of 12 BL individuals from CNGDC with project number PRJCA003284. We downloaded re-sequencing data of 24 individuals of an indigenous chicken (Daweishan chicken) (*Gallus gallus*) breed[67] from the NCBI SRA database with project number PRJNA893352.

Ethics approval

All the experimental procedures were approved by the Animal Care and Use Committee of the Yunnan Agricultural University (approval ID: YAU202103047). The care and use of animals fully complied with local animal welfare laws, guidelines, and policies.

Real-time quantitative PCR (RT-qPCR) analysis

517 Three female adult WT individuals were collected from Diqing Tibet Autonomous Prefecture,
518 Yannan Province, China. The birds were killed by electric shock to unconsciousness followed by
519 neck artery bleeding. One to two grams of 20 tissues were aseptically collected from each
520 individual bird in a centrifuge tube within 20 mins after sacrifice and immediately frozen in
521 liquid nitrogen, then stored at -80°C until use. The collected tissues included chest muscle, leg
522 muscle, liver, kidney, lung, spleen, heart, cerebellum, brain cortex, ovary, glandular, pancreas,
523 abdominal fat, skin from chest, crops, rectum, cecum, duodenum, small intestine and gizzard.
524 Total RNA from each tissue sample was extracted using TaKaRa MiniBEST Universal RNA
525 Extraction Kit (TaKaRa Biotechnology Co., Ltd., Dalian, P. R. China) according to the vendor's
526 instructions. cDNA was synthetized from the total RNA by using a PrimeScript RT reagent Kit
527 (TaKaRa Biotechnology Co., Ltd., Dalian, P. R. China) following the vendor's instructions as
528 previously described[88]. RT-qPCR was performed using the Bio-Rad CFX96 real-time PCR
529 platform (Bio-Rad Laboratories, Inc.) and SYBR Green master mix (iQTM SYBRGreen® Supermix,
530 Dalian TaKaRa Biotechnology Co. Ltd.). We randomly selected 17 putative new genes for
531 validation. The primers of the 17 putative new genes and their annealing temperatures are
532 listed in Supplementary Note. The β-actin gene was used as a reference. Primers were
533 commercially synthesized (Shanghai Shenggong Biochemistry Company, P.R.C.). Each PCR
534 reaction was performed in 25 µl volumes containing 12.5 µl of iQ™ SYBR Green Supermix, 0.5 µl
535 (10 mM) of each primer, and 1 µl of cDNA. Detection of products was performed with the
536 following cycle profile: one cycle of 95 °C for 2 min, and 40 cycles of 95 °C for 15 s, the
537 annealing temperature (Supplementary Note) for 30 s, and 72 °C for 30 s, followed by a final
538 cycle of 72 °C for 10 min. The $2^{-\Delta Ct}$ method was used to analyze mRNA abundance. All tissues

539 were analyzed with three biological replicates and each biological replicate with five technical
540 replicates.

541 **Protein-coding gene annotation**

542 To annotate the protein-coding genes and pseudogenes in the WT and BR genomes, we used a
543 combination of reference-based and RNA-based method as previously described[89]. Briefly, for
544 the reference-based method, we used the CDSs of 53 well-represented avian genomes in NCBI
545 (Table S1) as the templates. We mapped all the CDSs isoforms of genes in the 53 genomes to
546 the assembly using Splign (2.0.0)[90] using default settings. For each template gene whose CDSs
547 could be mapped to the assembly, we concatenated all the mapped parts on the assembly. If
548 the CDSs of the template gene could be mapped to multiple loci on the assemblies, we chose
549 the locus with the highest mapping identity and checked whether the resulting concatenated
550 sequence formed an intact ORF (it had a length of an integer multiple of three and contained no
551 premature stop codon). If resulting concatenated sequence formed an intact ORF, we called the
552 locus an intact gene. If resulting concatenated sequence did not form an intact ORF, i.e. its
553 length was not an integer multiple of three and/or it contained a premature stop codon, we
554 mapped the Illumina DNA short reads from the same individual to the locus in the assembly
555 allowing no mismatch and gaps using bowtie (v2.4.1)[91] with default settings. If each nucleotide
556 position in the locus can be mapped by at least 10 short reads, we considered the locus as a
557 pseudogene; otherwise, we called it a partially supported gene since the pseudogenization
558 mutation might be caused by the sequencing errors in the assembly that cannot be corrected
559 by the polishing process.

560 For the RNA-based method, we first mapped all the RNA-seq reads from the 20 tissues
561 of WT (Table S3) and the three tissues of BR (Table S4) to the rRNA database SILVA_138[92] using
562 bowtie (v2.4.1)[91] with default settings, and filtered out the mapped reads. We then mapped the
563 unaligned reads to each genome using STAR (2.7.0c)[93] with default settings. As the *Crossoptilon*
564 species are closely related[35,36], here, we used a total of 23 RNA-seq datasets from both species
565 in annotating each genome to fully utilize the available data. Particularly, the datasets of BR
566 were collected from tissues (blood, developing primaries, and developing tail feathers) that
567 were not collected from WT, thus, they were complementary to facilitate gene finding. Based
568 on the mapped reads to each genome, we assembled transcripts using genome-guided method
569 in Trinity (2.8.5)[94] with default settings. Then we mapped the assembled transcripts to their
570 corresponding genome using Splign (2.0.0)[90] with default settings, and defined their gene
571 structures, and removed those that partially overlap the genes and pseudogenes predicted by
572 the reference-based method or the non-coding RNA genes (see below). For each unmapped
573 assembled transcripts, we found the longest ORF in it, and called it a protein-coding gene if it
574 was at least 300 bp long.
575 For completeness, we also annotated tRNA, miRNA, rRNA, snoRNA, telomerase RNA and
576 SRP RNA genes in each genome using infernal (1.1.2)[95] with the Rfam (v.14) database[96] as the
577 reference using default settings.
578 **Single nucleotide variants calling**
579 To call the variants in the populations of BL, BR, WT and Daweishan chicken, we first mapped
580 the short reads of each individual to the WT genome using BWA (0.7.17)[97] and SAMtools (1.9)[98]
581 using default settings, and then called the variants for each individual using GATK-

582 HaplotypeCaller (4.1.6)[99] using default settings and merged the variants of each individual from
583 the same species using GATK-CombineGVCFs (4.1.6)[99] using default settings. We removed the
584 SNPs with Quality by depth (QD) < 2, Fisher strand (FS) > 60, Root mean square mapping quality
585 (MQ) < 40, Strand odd ratio (SOR) > 3, Rank Sum Test for mapping qualities (MQRankSum) < -
586 12.5 and Rank Sum Test for site position within reads (ReadPosRankSum) < -8 and indels with
587 QD < 2, FS > 200, SOR > 10, Likelihood-based test for the consanguinity among samples
588 (InbreedingCoeff) < -0.8 and ReadPosRankSum < -20.

589 To calculate the fixation rate of the pseudogenes in the population of each species, we
590 called the SNPs in the pseudogenes of each species using the DNA short reads from the species'
591 population (n=10 for WT and n=41 for BR) using the same method mentioned above. The
592 annotated pseudogenes of each species were used as the reference for the SNP calling.

593 **PCA, ancestry, and introgression analyses**

594 The called biallelic SNPs in each species located in strong linkage disequilibrium blocks and
595 those with a MAF<0.05 were filtered. Principal component analysis (PCA) was performed on the
596 remaining SNPs using PLINK (1.90)[100] with default settings. The same SNPs were used to infer
597 the ancestral relationships of the three species using ADMIXTURE (1.3.0)[62] with default settings.
598 The results for the number of ancestral groups K = 2 and 3 were tested. The same SNPs were
599 used to infer possible gene introgression among the three species by computing the D-statistic
600 using Dsuite[63] with default settings and the f3-statistic using ADMIXTOOLS[64] with default
601 settings.

602 **Calculation of allele frequencies of pseudogenes**

603 We computed allele frequencies of the first pseudogenization mutation of each pseudogene in

604 each species using GATK (4.1.6)[99] based on called SNPs and indels.

605 **Selective sweeps detection**

606 Selective sweeps in a species relative to another were detected using two methods including

607 genetic differentiation (F_{ST})[101] and difference in nucleotide diversity ($\Delta\pi$)[68]. These two methods

608 were widely used to detect selective sweeps by many studies[65-68]. We estimated F_{ST} for each

609 pair of comparison using VCFtools (0.1.16)[102] with a sliding window of 40 kb and a step size of

610 20 kb with default settings. We estimated π for each species using VCFtools (0.1.16)[102] with a

611 sliding window of 40 kb and a step size of 20 kb with default settings, and calculated the

612 difference in nucleotide diversity ($\Delta\pi$) in each window for each pair of comparison. To evaluate

613 the statistical significance of the F_{ST} and π values for a comparison, we generated a Null model

614 by shuffling the allele frequency data for 100 times while keeping the SNP positions fixed[69]. We

615 then computed F_{ST} and $\Delta\pi$ for the permuted windows as well as their means ($\mu(F_{ST_{Null}})$ and

616 $\mu(\Delta\pi_{Null})$) and standard deviations ($\sigma(F_{ST_{Null}})$ and $\sigma(\Delta\pi_{Null})$). We computed the Z value for

617 each F_{ST} and $\Delta\pi$ value for the comparison by using the following formulas:

618 $ZF_{ST}(i) = (F_{ST}(i) - \mu(F_{ST_{Null}}))/\sigma(F_{ST_{Null}})$ and

619 $Z\Delta\pi(i) = (\Delta\pi(i) - \mu(\Delta\pi_{Null}))/\sigma(\Delta\pi_{Null})$.

620 We considered a window with $ZF_{ST} > \alpha$ and $Z\Delta\pi > \beta$ or $Z\Delta\pi < -\beta$ ($\alpha>0$, $\beta>0$) as a

621 selective sweep. For the selective sweeps in each pair of comparison, we used the value of $Z\Delta\pi$

622 to help identify the selective sweeps of each species. Windows with $Z\Delta\pi$ scores < -β represent

623 selective sweeps of the minuend species, and windows with $Z\Delta\pi$ scores > β represent selective

624 sweeps of the subtrahend species. We set α = 2.33 and β = 1.64, corresponding to a one-tailed

625 and a two-tailed z-test, respectively.

626 **Runs of homozygosity (ROH) analysis**

627 ROH analysis in each species was done using BCFtools (1.10)[103] with the default settings based

628 on the SNPs called in each individual bird of the species.

629 **Tajima's D value calculations**

630 Tajima's D in each species was calculated using ANGSD (0.930)[104] with default settings based on

631 the SNPs called in each individual bird of the species.

632 **RNA-seq data analyses**

633 RNA-seq reads of each tissue were mapped to the WT or BR genome using STAR (2.7.0c)[93] with

634 default settings. The expression level of each gene or pseudogene g_i in the tissue was

635 computed as TPM (transcript per million), defined as $TPM_i = \frac{r_i/l_i}{\sum_j r_j/l_j} * 10^6$, where r_i denotes

636 reads mapped to g_i, l_i is the length of g_i, and $\sum_j r_j/l_j$ corresponds to the sum of mapped reads

637 to each g_j normalized by its length.

638 **Hierarchical clustering of gene expression levels**

639 The expression level of each gene g_i in a tissue was rescaled as $s_i = \frac{e_{i-}e_{min}}{e_{max-}e_{min}}$,

640 where e_i denotes the expression level of g_i, and e_{min} and e_{max} the minimal and maximal

641 expression levels of all genes in the tissue, respectively. The clustermap program from seaborn

642 in Python was used to generate the heatmaps in Figure 1.

643 **Data Availability**

644 The WT genome is available at GenBank with accession number GCA_036346035.1; the BR
645 genome is available at CNGDC with accession number GWHAOPW00000000; re-sequencing
646 data of 10 WT individuals are available at NCBI SRA with accession number SRP433016; re-

sequencing data of 41 BR individuals are available at CNGDC with project number PRJCA003284; re-sequencing data of 12 BL individuals are available at CNGDC with project number PRJCA003284 and at NCBI SRA with accession number SRP471294; RNA-seq data from 20 tissues of the WT individual are available at NCBI SRA with accession number SRP432961; RNA-seq data from the BR individual's blood, developing primaries and developing tail feathers tissues are available at CNGDC with project number PRJCA003284. Our gene annotation results of the WT and BR genomes are available at FigShare (https://doi.org/10.6084/m9.figshare.24438295.v1).

Code Availability

All gene annotation code and the corresponding pipeline description are available at https://github.com/zhengchangsulab/A-genome-assebmly-and-annotation-pipeline.

Author Contributions

CG, JJ, ZS and TD supervised and conceived the project; KW, XG and DW collected tissue samples and conducted molecular biology experiments; SW and SY assembled and annotated the genomes; SW and ZS performed data analysis; and SW and ZS wrote the manuscript.

Competing interests

The authors declare that they have no competing interests.

Funding

This work was supported by the National Natural Science Foundation of China (U2002205 and U1702232), Yunling Scholar Training Program of Yunnan Province (2014NO48), Yunling Industry and Technology Leading Talent Training Program of Yunnan Province (YNWR-CYJS-2015-027), Natural Science Foundation of Yunnan Province (2019IC008 and 2016ZA008), and Department of Bioinformatics and Genomics of the University of North Carolina at Charlotte.

References

1 Zhang, P. *et al.* Denisovans and Homo sapiens on the Tibetan Plateau: dispersals and adaptations. *Trends Ecol Evol* **37**, 257-267 (2022). https://doi.org:10.1016/j.tree.2021.11.004

2 Peng, Y. *et al.* Genetic variations in Tibetan populations and high-altitude adaptation at the Himalayas. *Mol Biol Evol* **28**, 1075-1081 (2011). https://doi.org:10.1093/molbev/msq290

3 Hu, H. *et al.* Evolutionary history of Tibetans inferred from whole-genome sequencing. *PLoS Genet* **13**, e1006675 (2017). https://doi.org:10.1371/journal.pgen.1006675

4 Wang, M. S. *et al.* Genomic Analyses Reveal Potential Independent Adaptation to High Altitude in Tibetan Chickens. *Mol Biol Evol* **32**, 1880-1889 (2015). https://doi.org:10.1093/molbev/msv071

5 Li, S. *et al.* A non-synonymous SNP with the allele frequency correlated with the altitude may contribute to the hypoxia adaptation of Tibetan chicken. *PLoS One* **12**, e0172211 (2017). https://doi.org:10.1371/journal.pone.0172211

6 Yuan, J. *et al.* Genome-wide run of homozygosity analysis reveals candidate genomic regions associated with environmental adaptations of Tibetan native chickens. *BMC Genomics* **23**, 91 (2022). https://doi.org:10.1186/s12864-021-08280-z

7 Li, M. *et al.* Genomic analyses identify distinct patterns of selection in domesticated pigs and Tibetan wild boars. *Nat.Genet* **45**, 1431-1438 (2013). https://doi.org:10.1038/ng.2811

8 Zhang, B. *et al.* Comparative transcriptomic and proteomic analyses provide insights into the key genes involved in high-altitude adaptation in the Tibetan pig. *Sci Rep* **7**, 3654 (2017). https://doi.org:10.1038/s41598-017-03976-3

9 Li, C. *et al.* Markhor-derived Introgression of a Genomic Region Encompassing PAPSS2 Confers High-altitude Adaptability in Tibetan Goats. *Mol Biol Evol* **39** (2022). https://doi.org:10.1093/molbev/msac253

10 Hu, X. J. *et al.* The Genome Landscape of Tibetan Sheep Reveals Adaptive Introgression from Argali and the History of Early Human Settlements on the Qinghai-Tibetan Plateau. *Mol Biol Evol* **36**, 283-303 (2019). https://doi.org:10.1093/molbev/msy208

11 Liu, J. *et al.* Genetic signatures of high-altitude adaptation and geographic distribution in Tibetan sheep. *Sci Rep* **10**, 18332 (2020). https://doi.org:10.1038/s41598-020-75428-4

12 Li, Y. *et al.* Population variation revealed high-altitude adaptation of Tibetan mastiffs. *Mol Biol Evol* **31**, 1200-1205 (2014). https://doi.org:10.1093/molbev/msu070

13 Wu, D. D. *et al.* Pervasive introgression facilitated domestication and adaptation in the Bos species complex. *Nature ecology & evolution* **2**, 1139-1145 (2018). https://doi.org:10.1038/s41559-018-0562-y

14 Simonson, T. S., McClain, D. A., Jorde, L. B. & Prchal, J. T. Genetic determinants of Tibetan high-altitude adaptation. *Hum Genet* **131**, 527-533 (2012). https://doi.org:10.1007/s00439-011-1109-3

15 Qu, Y. *et al.* Ground tit genome reveals avian adaptation to living at high altitudes in the Tibetan plateau. *Nat Commun* **4**, 2071 (2013). https://doi.org:10.1038/ncomms3071

16 Qiu, Q. *et al.* The yak genome and adaptation to life at high altitude. *Nat.Genet* **44**, 946-949 (2012). https://doi.org:10.1038/ng.2343

17 Simonson, T. S. *et al.* Genetic evidence for high-altitude adaptation in Tibet. *Science* **329**, 72-75 (2010). https://doi.org:10.1126/science.1189406

18 Ji, L. D. *et al.* Genetic adaptation of the hypoxia-inducible factor pathway to oxygen pressure among eurasian human populations. *Mol Biol Evol* **29**, 3359-3370 (2012). https://doi.org:10.1093/molbev/mss144

19 Xiong, Y. *et al.* Physiological and genetic convergence supports hypoxia resistance in high-altitude songbirds. *PLoS Genet* **16**, e1009270 (2020). https://doi.org:10.1371/journal.pgen.1009270

20 Peng, Y. *et al.* Down-Regulation of EPAS1 Transcription and Genetic Adaptation of Tibetans to High-Altitude Hypoxia. *Mol Biol Evol* **34**, 818-830 (2017). https://doi.org:10.1093/molbev/msw280

21 Xin, J. *et al.* Chromatin accessibility landscape and regulatory network of high-altitude hypoxia adaptation. *Nat Commun* **11**, 4928 (2020). https://doi.org:10.1038/s41467-020-18638-8

22 Xu, D. *et al.* A single mutation underlying phenotypic convergence for hypoxia adaptation on the Qinghai-Tibetan Plateau. *Cell Res* **31**, 1032-1035 (2021). https://doi.org:10.1038/s41422-021-00517-6

23 Zhu, X. *et al.* Divergent and parallel routes of biochemical adaptation in high-altitude passerine birds from the Qinghai-Tibet Plateau. *Proc Natl Acad Sci U S A* **115**, 1865-1870 (2018). https://doi.org:10.1073/pnas.1720487115

24 Guo, Y. B. *et al.* GCH1 plays a role in the high-altitude adaptation of Tibetans. *Zool Res* **38**, 155-162 (2017). https://doi.org:10.24272/j.issn.2095-8137.2017.037

25 Heinrich, E. C. *et al.* Genetic variants at the EGLN1 locus associated with high-altitude adaptation in Tibetans are absent or found at low frequency in highland Andeans. *Annals of human genetics* **83**, 171-176 (2019). https://doi.org:10.1111/ahg.12299

26 Xiang, K. *et al.* Identification of a Tibetan-specific mutation in the hypoxic gene EGLN1 and its contribution to high-altitude adaptation. *Mol Biol Evol* **30**, 1889-1898 (2013). https://doi.org:10.1093/molbev/mst090

27 Jeong, C. *et al.* Admixture facilitates genetic adaptations to high altitude in Tibet. *Nat Commun* **5**, 3281 (2014). https://doi.org:10.1038/ncomms4281

28 Li, D. *et al.* Population genomics identifies patterns of genetic diversity and selection in chicken. *BMC Genomics* **20**, 263 (2019). https://doi.org:10.1186/s12864-019-5622-4

29 Liu, X., Wang, X., Liu, J., Wang, X. & Bao, H. Identifying Candidate Genes for Hypoxia Adaptation of Tibet Chicken Embryos by Selection Signature Analyses and RNA Sequencing. *Genes* **11** (2020). https://doi.org:10.3390/genes11070823

30 Tang, Q. *et al.* HIF-1 regulates energy metabolism of the Tibetan chicken brain during embryo development under hypoxia. *Am J Physiol Regul Integr Comp Physiol* **320**, R704-r713 (2021). https://doi.org:10.1152/ajpregu.00052.2020

31 Zhang, Y., Zhang, H., Zhang, B., Ling, Y. & Zhang, H. Identification of key HIF-1α target genes that regulate adaptation to hypoxic conditions in Tibetan chicken embryos. *Gene* **729**, 144321 (2020). https://doi.org:10.1016/j.gene.2019.144321

32 Scheinfeldt, L. B. & Tishkoff, S. A. Living the high life: high-altitude adaptation. *Genome Biol* **11**, 133 (2010). https://doi.org:10.1186/gb-2010-11-9-133

33 Pamenter, M. E., Hall, J. E., Tanabe, Y. & Simonson, T. S. Cross-Species Insights Into Genomic Adaptations to Hypoxia. *Front Genet* **11**, 743 (2020). https://doi.org:10.3389/fgene.2020.00743

34 Friedrich, J. & Wiener, P. Selection signatures for high-altitude adaptation in ruminants. *Anim Genet* **51**, 157-165 (2020). https://doi.org:10.1111/age.12900

35 Li, X., Huang, Y. & Lei, F. Comparative mitochondrial genomics and phylogenetic relationships of the Crossoptilon species (Phasianidae, Galliformes). *BMC Genomics* **16**, 42 (2015). https://doi.org:10.1186/s12864-015-1234-9

36 Li, X. *et al.* Assessment of genetic diversity in Chinese eared pheasant using fluorescent-AFLP markers. *Mol Phylogenet Evol* **57**, 429-433 (2010). https://doi.org:10.1016/j.ympev.2010.05.024

37 Pang, X., Ma, J. & Liu, W. The research of the main variables of habitat selection in brown eared-pheasant breeding in XiaoWutai Mountain. *Journal of Hebei Forestry Science and Technology* **(Supplementary Issue)**, 27-29 (2009).

38 Zhao, Z. *Ornithology of China (Non-Passeriformes)*. Vol. 1 376-381 (Jilin Science and Technology Press, 2001).
39 Xu, Z., Lei, Y., Jin, X. & Yuan, H. Brown eared-pheasant population was found in Huanglong Mountain, Shanxi. *Chinese Wildlife* **19**, 13 (1998).
40 TH, C. *et al. Fauna of China*. Vol. IV 106–107 (Beijing: Science Press, 1978).
41 *Crossoptilon harmani IUCN Red List of Threatened Species*, 2016).
42 Li, Y., Li, X., Song, Z. & Ding, C. Determining the distribution loss of brown eared-pheasant (Crossoptilon mantchuricum) using historical data and potential distribution estimates. *PeerJ* **4**, e2556 (2016). https://doi.org:10.7717/peerj.2556
43 Wang, P. *et al.* The role of niche divergence and geographic arrangement in the speciation of Eared Pheasants (Crossoptilon, Hodgson 1938). *Mol Phylogenet Evol* **113**, 1-8 (2017). https://doi.org:10.1016/j.ympev.2017.05.003
44 Zheng, Z. *A complete checklist of species and subspecies of the Chinese birds*. (Science Press, 1994).
45 Wang, P. *et al.* Genomic Consequences of Long-Term Population Decline in Brown Eared Pheasant. *Mol Biol Evol* **38**, 263-273 (2021). https://doi.org:10.1093/molbev/msaa213
46 Wu, S. *et al.* High-quality genome assembly of a C. crossoptilon and related functional and genetics data resources. *Sci Data* **11**, 247 (2024). https://doi.org:10.1038/s41597-024-03087-5
47 Wu, S. De Novo Assemblies of Genomes of Four Indigenous Chickens and a White Eared Pheasant Reveal Genetic Basis of Chicken Domestication and Altitude Adaptation. *Dissertation* (2023). https://doi.org:https://graduateschool.charlotte.edu/de-novo-assemblies-genomes-four-indigenous-chickens-and-white-eared-pheasant-reveal-genetic-basis/
48 Sayers, E. W. *et al.* Database resources of the national center for biotechnology information. *Nucleic Acids Res* **50**, D20-d26 (2022). https://doi.org:10.1093/nar/gkab1112
49 Lovell, P. V. *et al.* Conserved syntenic clusters of protein coding genes are missing in birds. *Genome Biol* **15**, 565 (2014). https://doi.org:10.1186/s13059-014-0565-1
50 Zhang, Z. D., Frankish, A., Hunt, T., Harrow, J. & Gerstein, M. Identification and analysis of unitary pseudogenes: historic and contemporary gene losses in humans and other primates. *Genome Biol* **11**, R26 (2010). https://doi.org:10.1186/gb-2010-11-3-r26
51 Derks, M. F. L. *et al.* A survey of functional genomic variation in domesticated chickens. *Genet Sel Evol* **50**, 17 (2018). https://doi.org:10.1186/s12711-018-0390-1
52 Parmley, J. L. & Hurst, L. D. How do synonymous mutations affect fitness? *Bioessays* **29**, 515-519 (2007). https://doi.org:10.1002/bies.20592
53 Ng, P. C. *et al.* Genetic variation in an individual human exome. *PLoS Genet* **4**, e1000160 (2008). https://doi.org:10.1371/journal.pgen.1000160
54 Semenza, G. L. Targeting HIF-1 for cancer therapy. *Nat Rev Cancer* **3**, 721-732 (2003). https://doi.org:10.1038/nrc1187
55 Giaccia, A., Siim, B. G. & Johnson, R. S. HIF-1 as a target for drug development. *Nat Rev Drug Discov* **2**, 803-811 (2003). https://doi.org:10.1038/nrd1199
56 Bárdos, J. I. & Ashcroft, M. Hypoxia-inducible factor-1 and oncogenic signalling. *Bioessays* **26**, 262-269 (2004). https://doi.org:10.1002/bies.20002

57 Matsumoto, T. & Claesson-Welsh, L. VEGF receptor signal transduction. *Sci STKE* **2001**, re21 (2001). https://doi.org:10.1126/stke.2001.112.re21

58 Cross, M. J., Dixelius, J., Matsumoto, T. & Claesson-Welsh, L. VEGF-receptor signal transduction. *Trends Biochem Sci* **28**, 488-494 (2003). https://doi.org:10.1016/s0968-0004(03)00193-2

59 Ferrara, N., Gerber, H. P. & LeCouter, J. The biology of VEGF and its receptors. *Nat Med* **9**, 669-676 (2003). https://doi.org:10.1038/nm0603-669

60 Chatterjee, O. *et al.* An overview of the oxytocin-oxytocin receptor signaling network. *J Cell Commun Signal* **10**, 355-360 (2016). https://doi.org:10.1007/s12079-016-0353-7

61 Siwen Wu, K. W., Tengfei Dou, Sisi Yuan, Dong-Dong Wu, Changrong Ge, Junjing Jia,Zhengchang Su. High-quality genome assembly of a white eared pheasant individual and related functional and genetics data resources. *BioRxiv* (2023). https://doi.org:https://www.biorxiv.org/content/10.1101/2023.11.09.566452v1

62 Alexander, D. H., Novembre, J. & Lange, K. Fast model-based estimation of ancestry in unrelated individuals. *Genome Res* **19**, 1655-1664 (2009). https://doi.org:10.1101/gr.094052.109

63 Malinsky, M., Matschiner, M. & Svardal, H. Dsuite - Fast D-statistics and related admixture evidence from VCF files. *Mol Ecol Resour* **21**, 584-595 (2021). https://doi.org:10.1111/1755-0998.13265

64 Patterson, N. *et al.* Ancient admixture in human history. *Genetics* **192**, 1065-1093 (2012). https://doi.org:10.1534/genetics.112.145037

65 Wang, Y. M. *et al.* Integrating Genomic and Transcriptomic Data to Reveal Genetic Mechanisms Underlying Piao Chicken Rumpless Trait. *Genomics Proteomics Bioinformatics* **19**, 787-799 (2021). https://doi.org:10.1016/j.gpb.2020.06.019

66 Qanbari, S. *et al.* Genetics of adaptation in modern chicken. *PLoS Genet* **15**, e1007989 (2019). https://doi.org:10.1371/journal.pgen.1007989

67 Wu, S. *et al.* Artificial selection footprints in indigenous and commercial chicken genomes. *BMC Genomics* **25**, 428 (2024). https://doi.org:10.1186/s12864-024-10291-5

68 Wang, M. S. *et al.* Positive selection rather than relaxation of functional constraint drives the evolution of vision during chicken domestication. *Cell Res* **26**, 556-573 (2016). https://doi.org:10.1038/cr.2016.44

69 Churchill, G. A. & Doerge, R. W. Empirical threshold values for quantitative trait mapping. *Genetics* **138**, 963-971 (1994). https://doi.org:10.1093/genetics/138.3.963

70 Lelli, A. *et al.* Class III myosins shape the auditory hair bundles by limiting microvilli and stereocilia growth. *J Cell Biol* **212**, 231-244 (2016). https://doi.org:10.1083/jcb.201509017

71 Josep del Hoyo, A. E., Jordi Sargatal, David A Christie. *https://en.wikipedia.org/wiki/Handbook_of_the_Birds_of_the_World*, 1992).

72 Wu, L., Fu, J. & Shen, S. H. SKAP55 coupled with CD45 positively regulates T-cell receptor-mediated gene transcription. *Mol Cell Biol* **22**, 2673-2686 (2002). https://doi.org:10.1128/mcb.22.8.2673-2686.2002

73 D'Orléans-Juste, P., Plante, M., Honoré, J. C., Carrier, E. & Labonté, J. Synthesis and degradation of endothelin-1. *Can J Physiol Pharmacol* **81**, 503-510 (2003). https://doi.org:10.1139/y03-032

74 Neylon, C. B. Vascular biology of endothelin signal transduction. *Clin Exp Pharmacol Physiol* **26**, 149-153 (1999). https://doi.org:10.1046/j.1440-1681.1999.03013.x

75 Masaki, T., Miwa, S., Sawamura, T., Ninomiya, H. & Okamoto, Y. Subcellular mechanisms of endothelin action in vascular system. *Eur J Pharmacol* **375**, 133-138 (1999). https://doi.org:10.1016/s0014-2999(99)00252-6

76 Graham, A. M. & McCracken, K. G. Convergent evolution on the hypoxia-inducible factor (HIF) pathway genes EGLN1 and EPAS1 in high-altitude ducks. *Heredity (Edinb)* **122**, 819-832 (2019). https://doi.org:10.1038/s41437-018-0173-z

77 Martindale, J. L. & Holbrook, N. J. Cellular response to oxidative stress: signaling for suicide and survival. *J Cell Physiol* **192**, 1-15 (2002). https://doi.org:10.1002/jcp.10119

78 Davis, R. J. Signal transduction by the c-Jun N-terminal kinase. *Biochem Soc Symp* **64**, 1-12 (1999). https://doi.org:10.1515/9781400865048.1

79 Kyriakis, J. M. & Avruch, J. Mammalian mitogen-activated protein kinase signal transduction pathways activated by stress and inflammation. *Physiol Rev* **81**, 807-869 (2001). https://doi.org:10.1152/physrev.2001.81.2.807

80 Tibbles, L. A. & Woodgett, J. R. The stress-activated protein kinase pathways. *Cell Mol Life Sci* **55**, 1230-1254 (1999). https://doi.org:10.1007/s000180050369

81 Leppä, S. & Bohmann, D. Diverse functions of JNK signaling and c-Jun in stress response and apoptosis. *Oncogene* **18**, 6158-6162 (1999). https://doi.org:10.1038/sj.onc.1203173

82 Myung, P. S., Boerthe, N. J. & Koretzky, G. A. Adapter proteins in lymphocyte antigen-receptor signaling. *Curr Opin Immunol* **12**, 256-266 (2000). https://doi.org:10.1016/s0952-7915(00)00085-6

83 Krogsgaard, M., Huppa, J. B., Purbhoo, M. A. & Davis, M. M. Linking molecular and cellular events in T-cell activation and synapse formation. *Semin Immunol* **15**, 307-315 (2003). https://doi.org:10.1016/j.smim.2003.09.002

84 Kane, L. P., Lin, J. & Weiss, A. Signal transduction by the TCR for antigen. *Curr Opin Immunol* **12**, 242-249 (2000). https://doi.org:10.1016/s0952-7915(00)00083-2

85 Lukacs, N. W. Role of chemokines in the pathogenesis of asthma. *Nat Rev Immunol* **1**, 108-116 (2001). https://doi.org:10.1038/35100503

86 Vicente-Manzanares, M., Sancho, D., Yáñez-Mó, M. & Sánchez-Madrid, F. The leukocyte cytoskeleton in cell migration and immune interactions. *Int Rev Cytol* **216**, 233-289 (2002). https://doi.org:10.1016/s0074-7696(02)16007-4

87 Rhie, A. *et al.* Towards complete and error-free genome assemblies of all vertebrate species. *Nature* **592**, 737-746 (2021). https://doi.org:10.1038/s41586-021-03451-0

88 Zhao, J. *et al.* Transcriptomics reveals the molecular regulation of Chinese medicine formula on improving bone quality in broiler. *Poult Sci* **102**, 103044 (2023). https://doi.org:10.1016/j.psj.2023.103044

89 Wu, S. *et al.* Annotations of four high-quality indigenous chicken genomes identify more than one thousand missing genes in subtelomeric regions and micro-chromosomes with high G/C contents. *BMC Genomics* **25**, 430 (2024). https://doi.org:10.1186/s12864-024-10316-z

90 Kapustin, Y., Souvorov, A., Tatusova, T. & Lipman, D. Splign: algorithms for computing spliced alignments with identification of paralogs. *Biol Direct* **3**, 20 (2008). https://doi.org:10.1186/1745-6150-3-20

91 Langmead, B. & Salzberg, S. L. Fast gapped-read alignment with Bowtie 2. *Nat Methods* **9**, 357-359 (2012). https://doi.org:10.1038/nmeth.1923

92 Quast, C. *et al.* The SILVA ribosomal RNA gene database project: improved data processing and web-based tools. *Nucleic Acids Res* **41**, D590-596 (2013). https://doi.org:10.1093/nar/gks1219

93 Dobin, A. *et al.* STAR: ultrafast universal RNA-seq aligner. *Bioinformatics* **29**, 15-21 (2013). https://doi.org:10.1093/bioinformatics/bts635

94 Grabherr, M. G. *et al.* Full-length transcriptome assembly from RNA-Seq data without a reference genome. *Nat Biotechnol* **29**, 644-652 (2011). https://doi.org:10.1038/nbt.1883

95 Nawrocki, E. P. & Eddy, S. R. Infernal 1.1: 100-fold faster RNA homology searches. *Bioinformatics* **29**, 2933-2935 (2013). https://doi.org:10.1093/bioinformatics/btt509

96 Kalvari, I. *et al.* Rfam 14: expanded coverage of metagenomic, viral and microRNA families. *Nucleic Acids Res* **49**, D192-d200 (2021). https://doi.org:10.1093/nar/gkaa1047

97 Li, H. & Durbin, R. Fast and accurate short read alignment with Burrows-Wheeler transform. *Bioinformatics* **25**, 1754-1760 (2009). https://doi.org:10.1093/bioinformatics/btp324

98 Li, H. *et al.* The Sequence Alignment/Map format and SAMtools. *Bioinformatics* **25**, 2078-2079 (2009). https://doi.org:10.1093/bioinformatics/btp352

99 McKenna, A. *et al.* The Genome Analysis Toolkit: a MapReduce framework for analyzing next-generation DNA sequencing data. *Genome Res* **20**, 1297-1303 (2010). https://doi.org:10.1101/gr.107524.110

100 Chen, Z. L. *et al.* A high-speed search engine pLink 2 with systematic evaluation for proteome-scale identification of cross-linked peptides. *Nat Commun* **10**, 3404 (2019). https://doi.org:10.1038/s41467-019-11337-z

101 Reynolds, J., Weir, B. S. & Cockerham, C. C. Estimation of the coancestry coefficient: basis for a short-term genetic distance. *Genetics* **105**, 767-779 (1983). https://doi.org:10.1093/genetics/105.3.767

102 Danecek, P. *et al.* The variant call format and VCFtools. *Bioinformatics* **27**, 2156-2158 (2011). https://doi.org:10.1093/bioinformatics/btr330

103 Narasimhan, V. *et al.* BCFtools/RoH: a hidden Markov model approach for detecting autozygosity from next-generation sequencing data. *Bioinformatics* **32**, 1749-1751 (2016). https://doi.org:10.1093/bioinformatics/btw044

104 Korneliussen, T. S., Albrechtsen, A. & Nielsen, R. ANGSD: Analysis of Next Generation Sequencing Data. *BMC Bioinformatics* **15**, 356 (2014). https://doi.org:10.1186/s12859-014-0356-4

Table 1: Gene annotation of two *Crossoptilon* species, *C. crossoptilon* (WT) and *C. mantchuricum* (BR), using reference- and RNA-based methods

Breeds	Reference-based			RNA-based		# Total genes	# Total pseudogenes
	# Intact	# Partial	# Pseudogenes	# NT-supported	# Novel		
WT	14,815	750	1,519	751	61	16,377	1,519
BR	14,518	209	1,976	631	52	15,410	1,976
Common	14,057		1,040	422	28	14,507	1,040

Table 2: Numbers of SNPs identified in the *C. auritum* (BL), *C. mantchuricum* (BR) and *C. crossoptilon* (WT) populations

Breeds	# individuals	# Total SNPs
BL	12	10,147,889
BR	41	6,849,438
WT	10	9,004,245
All	63	16,459,558

Table 3: The f3-statistic and associated z-scores for the three choices of (target; source 1, source 2) among the three species

Source 1	Source 2	Target	f3	std. err	Z-score
WT	BR	BL	-0.0586	0.0022	-26.45
WT	BL	BR	1.2340	0.0769	16.04
BR	BL	WT	0.8392	0.0047	180.24

Table 4: Summary of selective sweeps (SS) and discrete selective sweeps (DSS) identified in pairwise comparisons between three *Crossoptilon* species populations

Comparison	BL			BR			WT		
	# SS (# DSS)	# Genes in DSS	# Pathways involved	# SS (# DSS)	# Genes in DSS	# Pathways involved	# SS (# DSS)	# Genes in DSS	# Pathways involved
BL vs. BR	208 (128)	143	48	638 (463)	474	56	NA	NA	NA
BL vs. WT	92 (72)	67	17	NA	NA	NA	274 (181)	167	34
BR vs. WT	NA	NA	NA	306 (184)	196	45	359 (188)	167	36

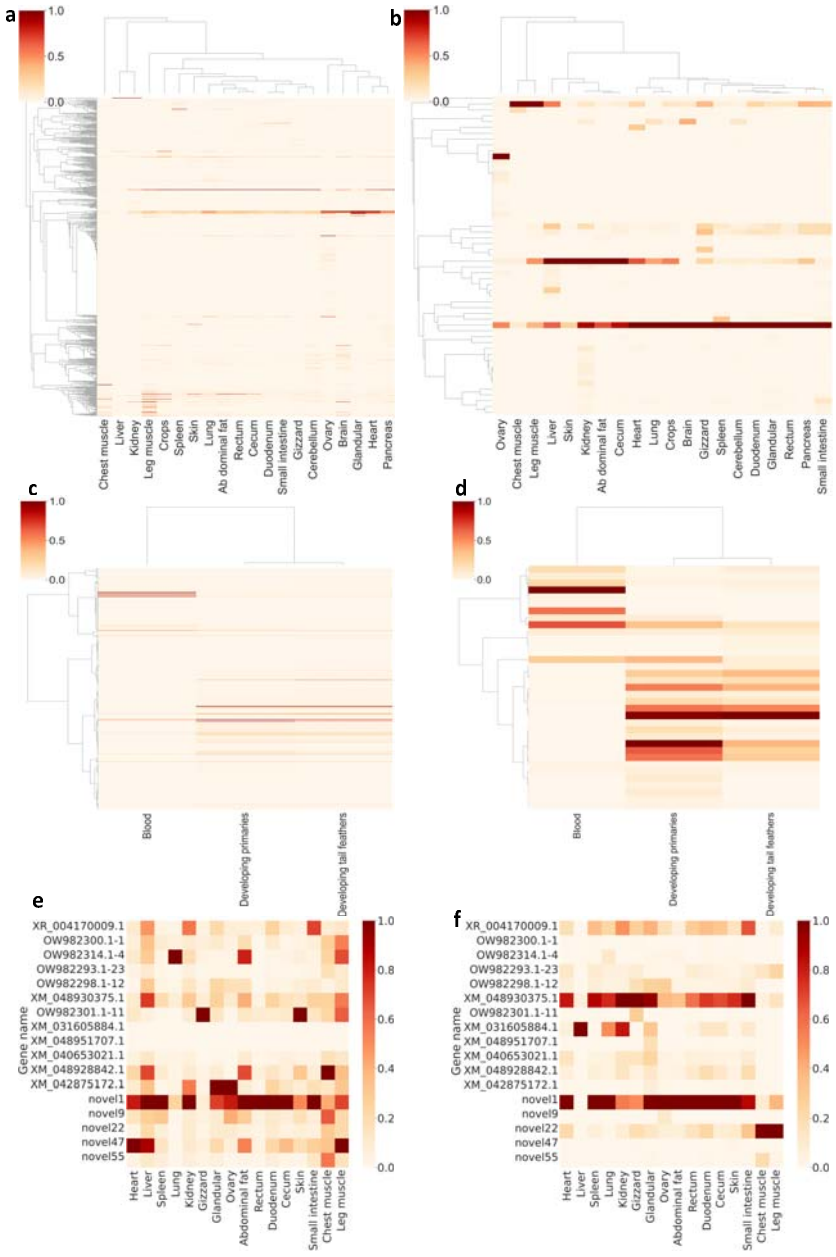

Figure 1. Heatmaps of expression levels of new genes in tissues of *C. crossoptilon* (WT) and *C. mantchuricum* (BR). **a.** Expression pattern of the NT-supported new genes in 20 tissues of WT. **b.** Expression pattern of the novel genes in 20 tissues of WT. **c.** Expression pattern of the NT-supported new genes in three tissues of BR. **d.** Expression pattern of the novel genes in three tissues in BR. **e.** Expression pattern of the 17 selected new genes in WT measured by RT-qPCR. **f.** Expression pattern of the 17 selected new genes quantified using RNA-seq data in WT. The expression levels of genes are scaled such that 0 represents a gene that was not expressed and 1 represents a gene that has the highest expression level in the tissue (Materials and Methods). Figures a-d and f were based on TPMs, and e was based on RT-qPCR results.

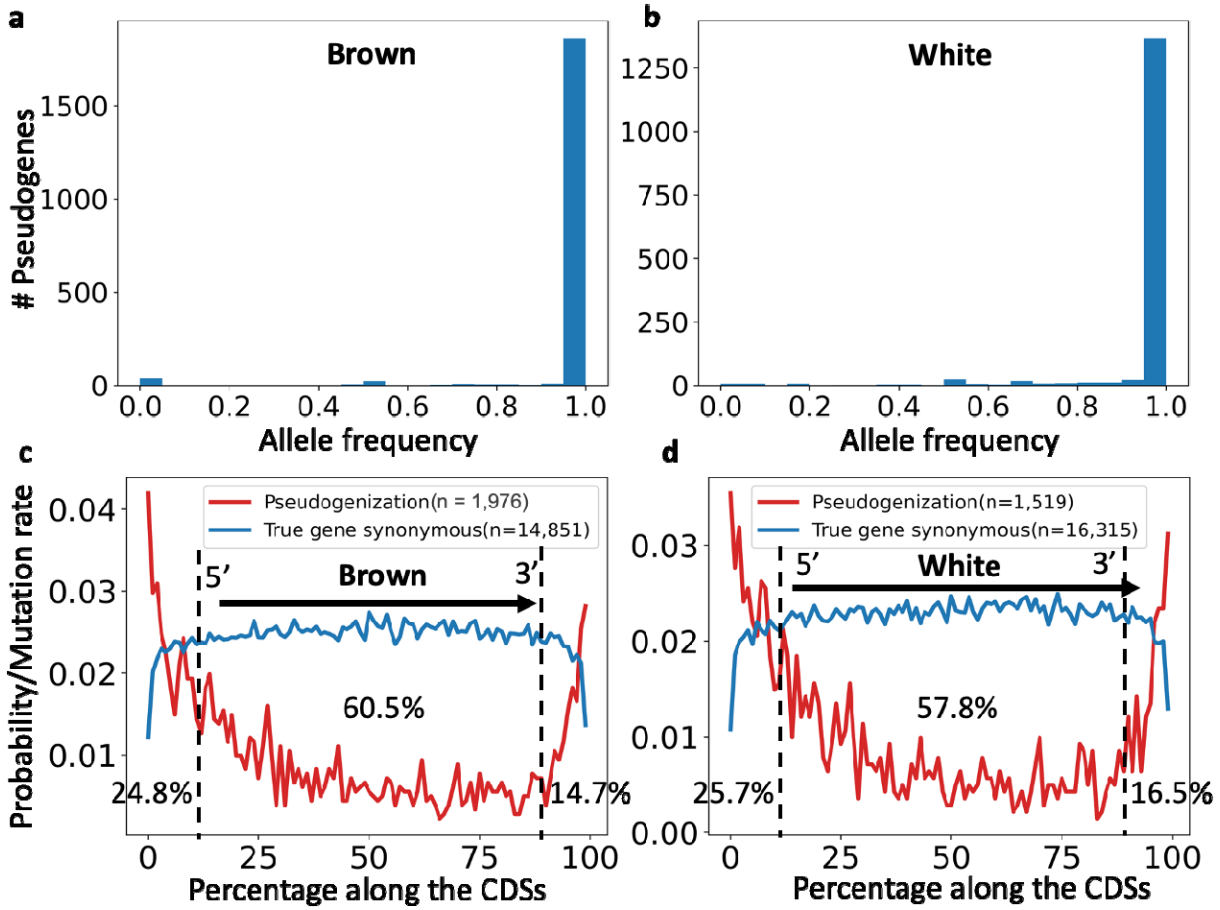

Figure 2. Fixation rate of pseudogenes in the WT and BR populations and distribution of the first pseudogenization alleles along the CDSs of parental genes. **a.** Number of pseudogenization alleles with indicated frequencies in the BR population. **b.** Number of the pseudogenization alleles with indicated frequencies in the WT populations. **c.** Distribution of the first pseudogenization alleles in the BR genome along the CDSs of parental genes. Notably, 24.8%, 60.5%, and 14.7% of the first pseudogenization alleles are in the first 10%, middle 80% and last 10% of the CDS regions. **d.** Distribution of the first pseudogenization alleles in the WT genome along the CDSs of parental genes. Notably, 25.7%, 57.8% and 16.5% of the first pseudogenization alleles are in the first 10%, middle 80% and last 10% of the CDS region.

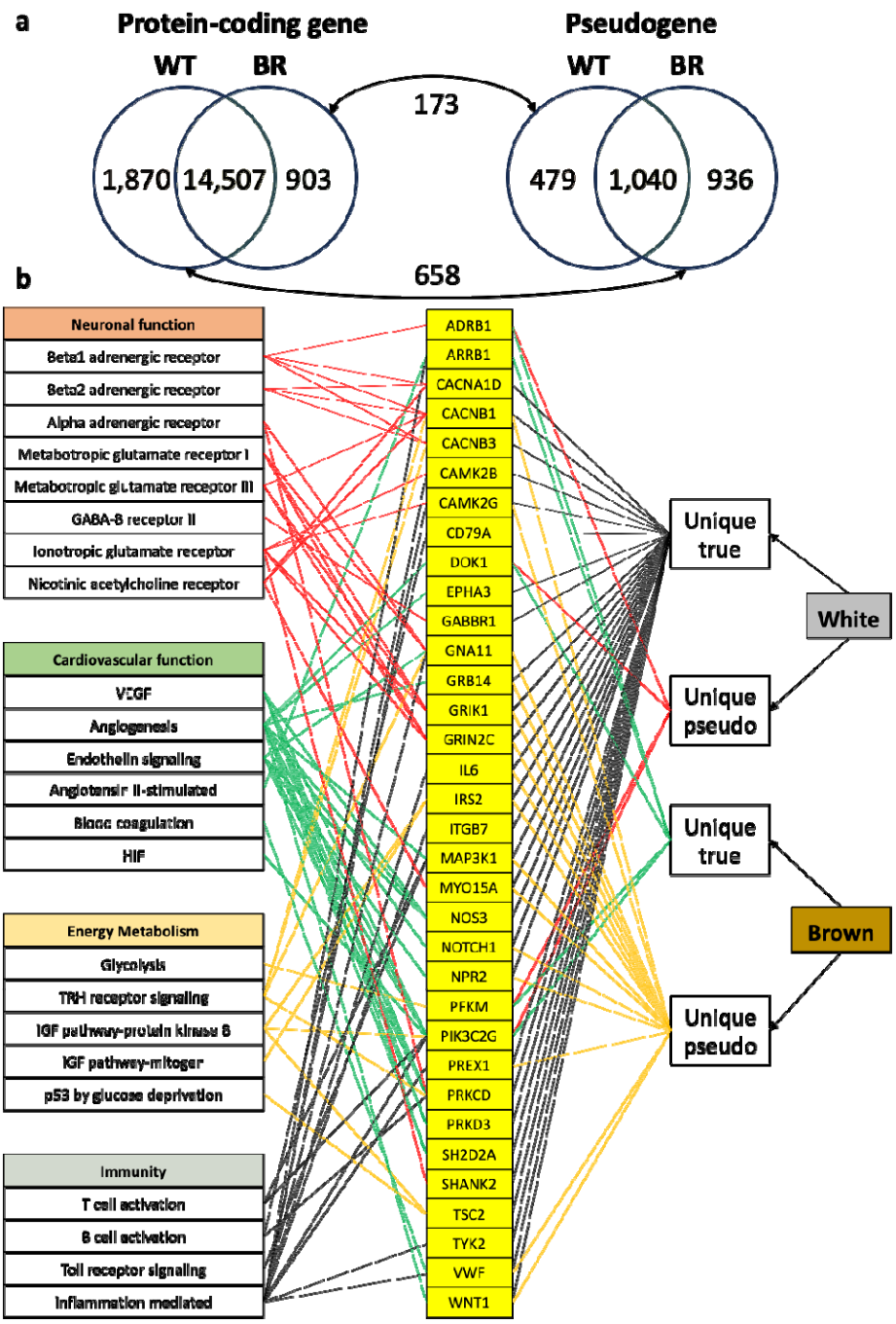

Figure 3. Functional analysis of the unique genes and pseudogene in the WT and BR genomes. **a.** Venn diagram showing shared and unique genes (left) and pseudogenes (right) in the two species. Of note, 658 WT genes are pseudogenized in BR and 173 BR genes are pseudogenized in WT, and there are a total of 3,357 non redundant unique genes and pseudogenes in the two genomes. **b.** The unique genes/pseudogenes in the WT and BR genomes that are involved in pathways related to four functional categories: neuronal functions, cardiovascular functions, energy metabolism, and immunity. Notably, unique genes in a species often became unique pseudogenes in the other species.

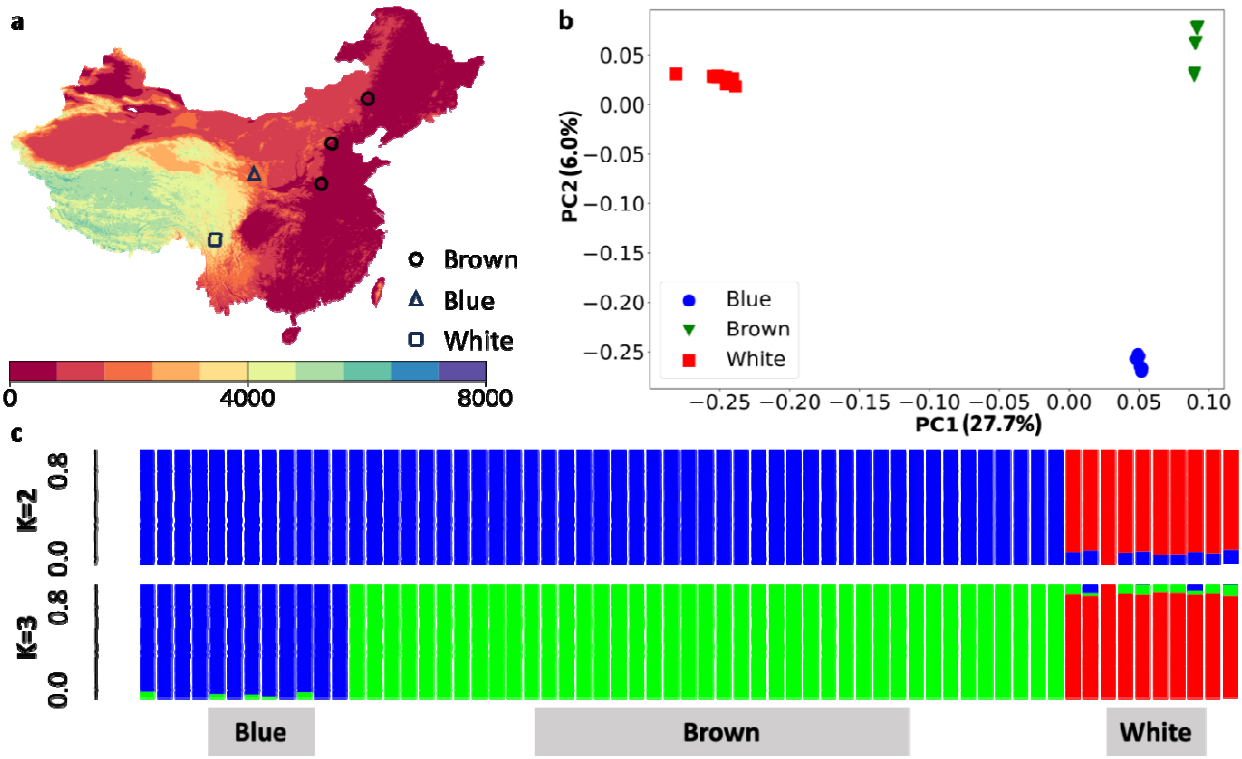

Figure 4. Geographic distribution and population structure of the WT, BL and BR populations. **a.** Geographic distribution of the three species used in this study. The color of the map indicates altitude level (m). **b.** Principal component analysis of the populations of the three species based on their SNP spectrum. **c.** Ancestral analysis of the individuals of the three species using ADMIXTURE for K=2 and 3.

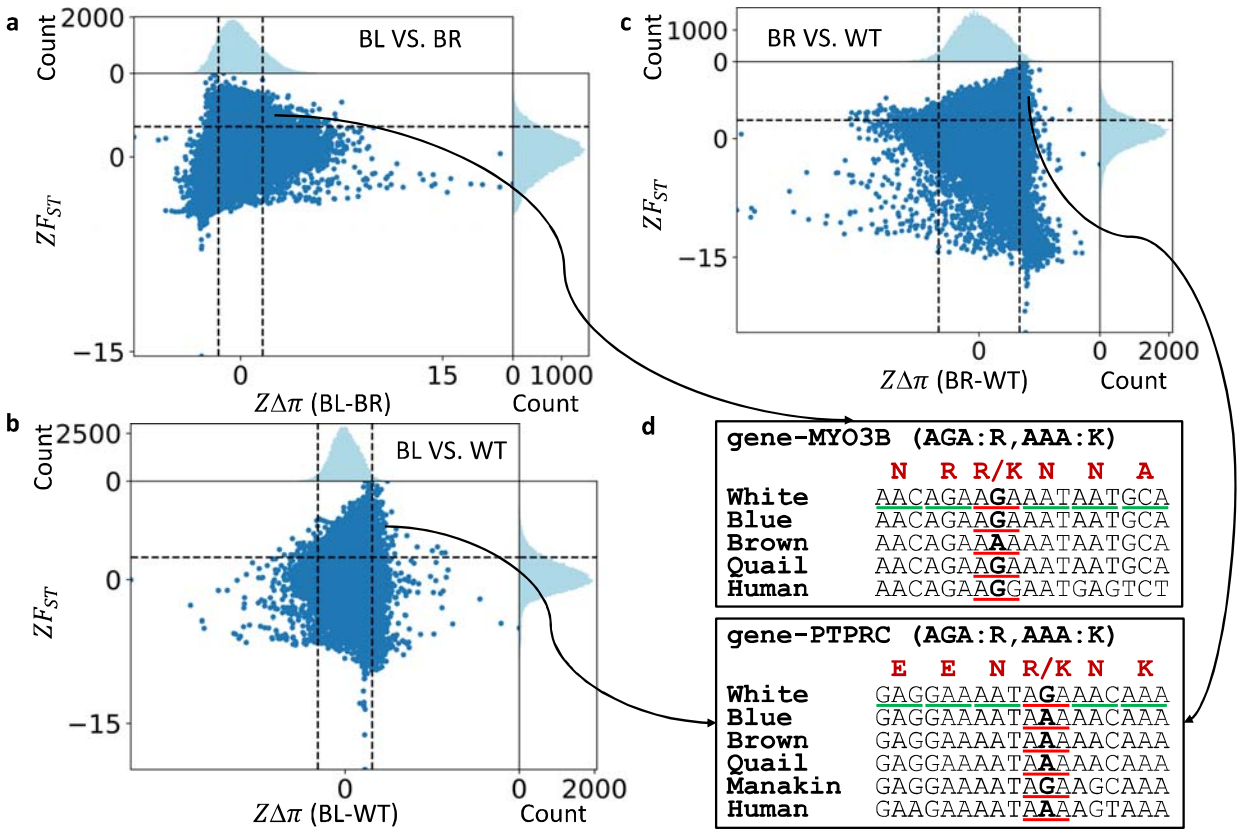

Figure 5. Distribution of the ZF_{ST} and $Z\Delta\pi$ values of each sliding window for the three pairwise comparisons. **a.** BL VS. BR comparison. **b.** BL VS. WT comparison. **c.** BR VS. WT comparison. **d.** Multiple alignments of part of CDSs of two genes in DSSs in different species. In subfigures a, b and c, the top panel represents the distribution of $Z\Delta\pi$ values and the bottom right one represents the distribution of ZF_{ST}values. Each dot in the bottom left panel represents a sliding window with its $Z\Delta\pi$ and ZF_{ST} values being its coordinates in the plot. The dashed lines represent the cut-offs for the ZF_{ST} and $Z\Delta\pi$ values.

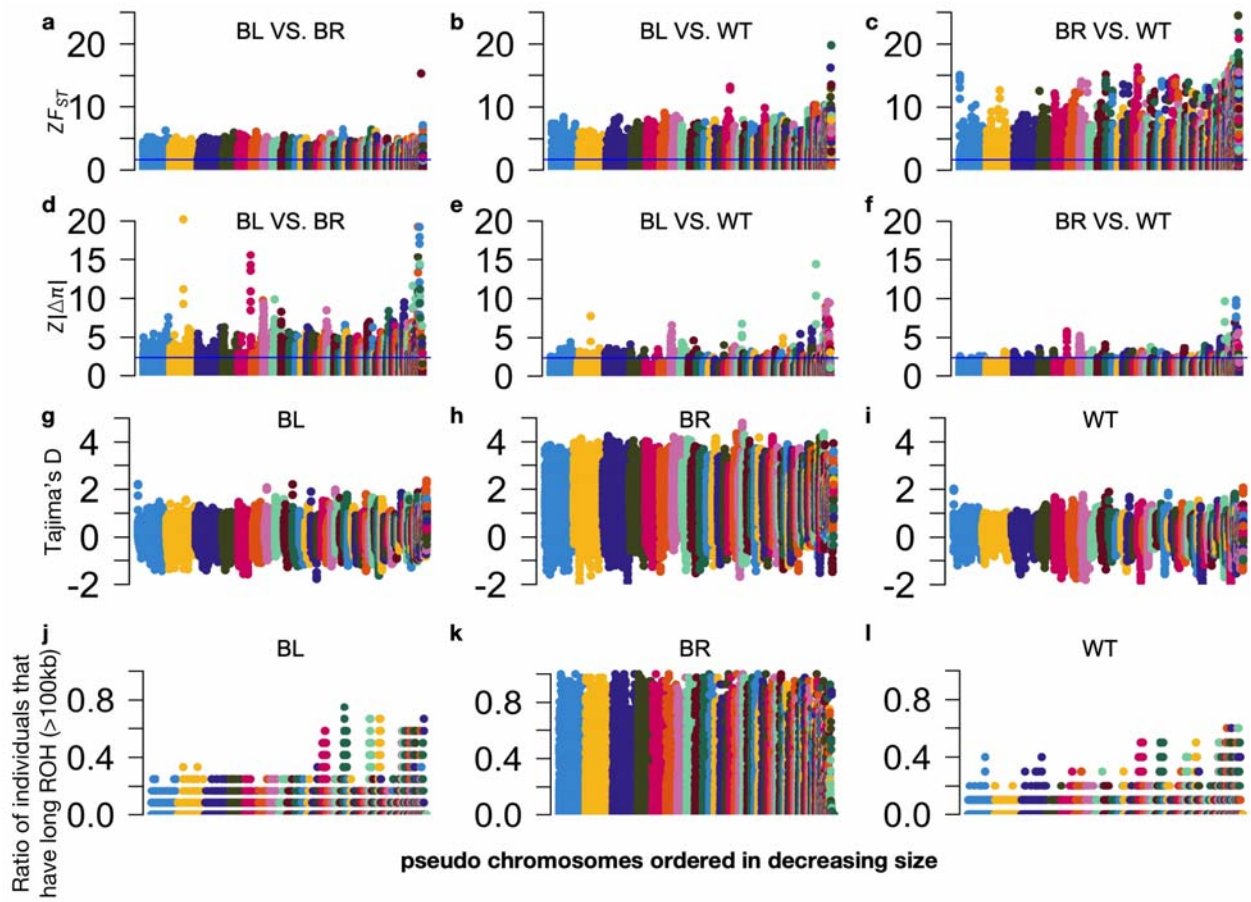

Figure 6. Manhattan plots for genome-wide analyses of the evolution of the three species. **a-c.** Manhattan plots of ZF_{ST} for the three pair-wise comparisons of the species. The blue line indicates the cut-off value. **d-f.** Manhattan plots of $Z|\Delta\pi|$ for the three pair-wise comparisons of the species. The blue line indicates the cut-off value. **g-i.** Manhattan plots of Tajima's D values for each species. **j-l.** Manhattan plots of the ratio of individuals that have long ROH (>100kb) for each species. In the figures, each dot represents a sliding window. The horizontal axes are pseudo chromosomes ordered in decreasing size.

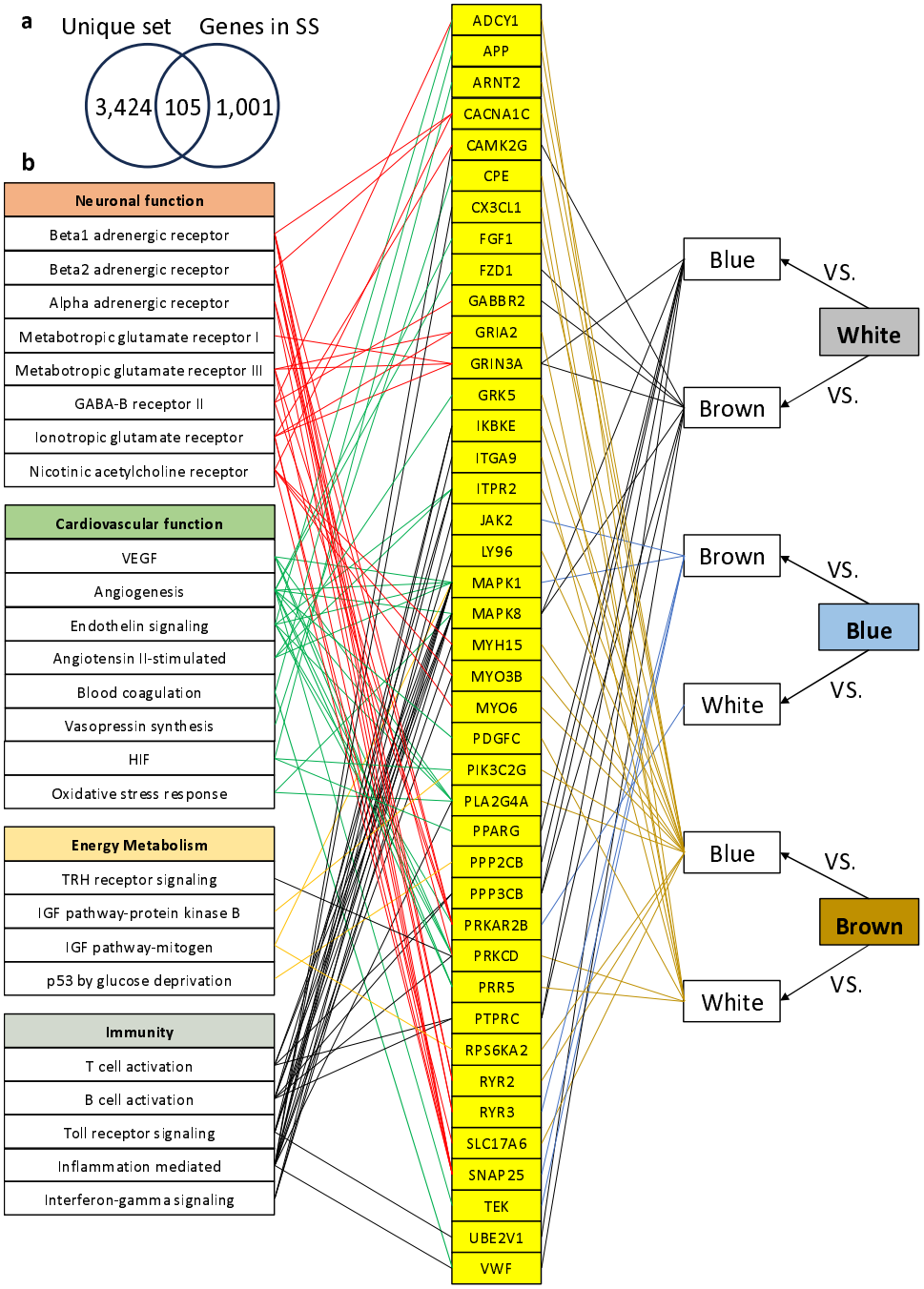

Figure 7. Comparison of unique genes and pseudogenes in the WT and BR genomes and genes in selective sweeps in the three species. **a.** Venn diagram of the set of unique genes and pseudogenes in the WT and BR genomes (unique set) and the set of genes in selective sweeps in the three species (genes in SS). **b.** The genes with GO term assignment in selection sweeps in each species that are involved in the same pathways of the same four functional categories as are the unique genes and unique pseudogenes with GO term assignment in the WT and BR genome, although the two sets only share four genes, i.e., *CAMK2G* and *VWF* are pseudogenized in BR, *PRKCD* is missing in BR, and *PIK3C2G* is pseudogenized in WT (Figure 3b).